MTL TR 92-35

COATED TUNGSTEN POWDERS FOR ADVANCED ORDNANCE APPLICATIONS, PHASE II, SBIR

May 1992

BRIAN E. WILLIAMS, JACOB J. STIGLICH, Jr., and RICHARD B. KAPLAN

Ultramet
12173 Montague Street
Pacoima, CA 91331

FINAL REPORT

Contract DAAL04-88-C-0030

Prepared for

U.S. ARMY MATERIALS TECHNOLOGY LABORATORY
Watertown, Massachusetts 02172-0001

The findings in this report are not to be construed as an official Department of the Army position, unless so designated by other authorized documents.

Mention of any trade names or manufacturers in this report shall not be construed as advertising nor as an official indorsement or approval of such products or companies by the United States Government.

DISPOSITION INSTRUCTIONS

Destroy this report when it is no longer needed.
Do not return it to the originator.

REPORT DOCUMENTATION PAGE

Form Approved
OMB No. 0704-0188

1a. REPORT SECURITY CLASSIFICATION Unclassified	1b. RESTRICTIVE MARKINGS N/A
2a. SECURITY CLASSIFICATION AUTHORITY N/A	3. DISTRIBUTION/AVAILABILITY OF REPORT Approved for public release; distribution unlimited.
2b. DECLASSIFICATION/DOWNGRADING SCHEDULE N/A	
4. PERFORMING ORGANIZATION REPORT NUMBER(S) ULT/TR-91-6821	5. MONITORING ORGANIZATION REPORT NUMBER(S)
6a. NAME OF PERFORMING ORGANIZATION Ultramet 6b. OFFICE SYMBOL (If applicable)	7a. NAME OF MONITORING ORGANIZATION
6c. ADDRESS (City, State, and ZIP Code) 12173 Montague Street Pacoima, CA 91331	7b. ADDRESS (City, State, and ZIP Code)
8a. NAME OF FUNDING/SPONSORING ORGANIZATION U.S. Army 8b. OFFICE SYMBOL (If applicable) SLCMT-PR	9. PROCUREMENT INSTRUMENT IDENTIFICATION NUMBER DAAL04-88-C-0030 MTL TR 92-35
8c. ADDRESS (City, State, and ZIP Code) Materials Technology Laboratory Watertown, MA 02172-0001	10. SOURCE OF FUNDING NUMBERS PROGRAM ELEMENT NO. / PROJECT NO. / TASK NO / WORK UNIT ACCESSION NO.

11. TITLE (Include Security Classification)

COATED TUNGSTEN POWDERS FOR ADVANCED ORDNANCE APPLICATIONS, PHASE II, SBIR

12. PERSONAL AUTHOR(S)

Brian E. Williams, Jacob J. Stiglich, Jr., and Richard B. Kaplan

13a. TYPE OF REPORT	13b. TIME COVERED	14. DATE OF REPORT (Year, Month, Day)	15. PAGE COUNT
Final Technical	FROM 9/88 TO 7/91	May 1992	67

16. SUPPLEMENTARY NOTATION

Small Business Innovation Research (SBIR) Program, Phase II

17. COSATI CODES			18. SUBJECT TERMS (Continue on reverse if necessary and identify by block number)
FIELD	GROUP	SUB-GROUP	
11	03		Tungsten powder, Composites, Chemical vapor deposition (CVD), Microstructure, Powder metallurgy
11	06	(01)	

19. ABSTRACT (Continue on reverse if necessary and identify by block number)

In this program, Ultramet optimized and characterized a fluidized-bed chemical vapor deposition (CVD) process for depositing nickel and iron onto tungsten particles for potential use as kinetic energy penetrator materials. The process yields a composite powder having the nominal composition W:6%Ni/Fe, in which the Ni:Fe ratio is 7:3. Two relatively narrow tungsten particle size distributions were used: one with a mean size of 12-15 μm, the other with a mean size of 5 μm. These particle sizes facilitated fluidized-bed CVD processing, but limited the ability to consolidate the materials by liquid phase sintering (LPS). Consequently, solid-state consolidation (Ceracon® process) was used to fabricate billets from which flexure, tensile, impact, and quarter-scale ballistic specimens could be machined. Initial three-point flexure measurements were very encouraging, with modulus-of-rupture values 30-50% higher than those of commercial (90:10, LPS) material cut into similar bars and tested concurrently, and midspan deflections equal to those of the (usually) more ductile 90:10 material. The tensile, impact, and ballistic properties of specimens (continued)

20. DISTRIBUTION/AVAILABILITY OF ABSTRACT ☒ UNCLASSIFIED/UNLIMITED ☐ SAME AS RPT. ☐ DTIC USERS	21. ABSTRACT SECURITY CLASSIFICATION Unclassified
22a. NAME OF RESPONSIBLE INDIVIDUAL Robert J. Dowding	22b. TELEPHONE (Include Area Code) 617-923-5340 / 22c. OFFICE SYMBOL SLCMT-MEM

Block 19 continued:
fabricated from larger billets, however, did not reproduce the earlier flexure results. Tensile strengths were respectable, but ductility was limited to ≤1% elongation. This brittleness was borne out in impact testing and in ballistic testing against spaced plate targets, although ballistic testing against semi-infinite rolled homogeneous armor at 0° obliquity yielded results identical to those for commercial and experimental tungsten composites of comparable density (tungsten content).

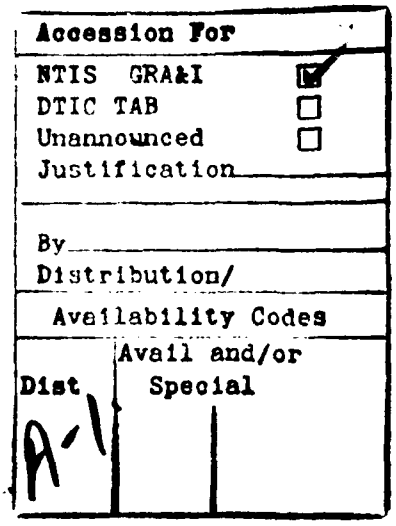

TABLE OF CONTENTS

LIST OF FIGURES

LIST OF FIGURES (cont.)

LIST OF TABLES

1. INTRODUCTION

This is the final technical report submitted by Ultramet, Pacoima, CA 91331 to the U.S. Army Materials Technology Laboratory, Watertown, MA 02172-0001 under SBIR Phase II contract DAAL04-88-C-0030. The period of this contract was from 30 September 1988 to 30 July 1991. The principal investigator was Richard B. Kaplan, supported by Brian E. Williams as project engineer and Jacob J. Stiglich Jr. as technical consultant. The AMTL program managers were Kenneth J. Tauer and Robert J. Dowding.

Depleted uranium (DU) alloys have been the primary materials used for kinetic energy penetrators by the U.S. Army, Navy, and Air Force. DU outperforms tungsten-based composites against all targets of interest to the Army and the Air Force, which is responsible for providing close air support for Army ground operations. Concerns about the environmental and political costs of DU materials, however, have accelerated the Army's investment in the development of an acceptable (i.e., capable of equivalent or better performance than DU) tungsten composite penetrator. The Navy has developed a 95-wt% tungsten composite that outperforms DU in the Phalanx close-in weapons system, and has begun replacing DU in its inventories; however, as of 1991, an acceptable tungsten composite penetrator continues to elude the Army/Air Force.

Tungsten materials development efforts have emphasized improvements in mechanical properties, but the improvements made have not yet translated into improved ballistic performance.

The developmental work performed in this program was intended to result in a more versatile and less costly powder preparation technology that ultimately would permit property/processing improvements for all particle-reinforced metal matrix and ceramic matrix composites. Research into penetration phenomena, meanwhile, has begun to detail the reasons for one material outperforming another. This research, combined with the powder production technology being developed by Ultramet, would permit the fabrication of more versatile materials having a wider range of property/processing capabilities.

In Phase I, Ultramet had developed a fluidized-bed chemical vapor deposition (CVD) process for applying Ni/Fe and Ni/Co as matrix materials to tungsten particles. The overall nominal composition was W:6%Ni/Fe (or Ni/Co), with a Ni:Fe or Ni:Co ratio of 7:3. The objectives of this Phase II program included the following:

- Optimize the CVD powder coating technology, the feasibility of which was demonstrated in Phase I for the deposition of Ni/Fe and Ni/Co onto tungsten particles.
- Scale up the CVD reactor capacity to a 5-kg batch size, from the 100- to 200-g capacity demonstrated in Phase I.
- Compare different consolidation techniques for the fabrication of billets from which physical and ballistic test specimens could be fabricated.

- Conduct mechanical property characterization and initial ballistic testing for comparison with commercial material (Teledyne-LPS) performance.

- Perform preliminary design and economic analysis of a 20-kg batch size reactor for prototype commercialization studies.

Coating development was successful in that the target compositions and Ni:Fe and Ni:Co ratios were achieved. Ni/Co codeposition was demonstrated early in Phase II, then discontinued in favor of the Ni/Fe matrix because of the prohibitive cost of the cobalt precursor.

Composite powders were consolidated by hot isostatic pressing (HIP) and by the Ceracon® process. Initial results of Ceracon consolidation were encouraging in that three-point flexure specimens taken from small billets exhibited strengths 30 to 50% greater than samples cut from commercial 90-wt% tungsten liquid phase sintered (LPS) material, which normally has higher flexure strengths than a 95-wt% tungsten LPS material. Midspan deflections for the Ultramet 94-wt% tungsten Ceracon material were approximately equivalent to those of the commercial 90-wt% tungsten LPS material, from which comparable ductility was inferred (another encouraging result).

These results were not repeatable, however, with specimens taken from larger billets processed in a similar manner to the smaller Ceracon-processed billets. Ballistic results for quarter-scale long rods fabricated from these larger billets, tested against spaced metal plate targets, were also not encouraging.

In summary, Ultramet demonstrated a powerful new technique for producing metal matrix composite powders free of dispersed phase contiguity and inhomogeneity at any composition. Both of these effects result from coating each particle with the precise matrix metal composition desired in the final bulk composite. Three-point flexure results for specimens cut from small billets showed significant improvements in strength and ductility over comparable LPS materials, but these results could not be repeated in specimens cut from larger billets. This indicates the need for further exploration of the processing/property relationships in the Ceracon consolidation process and their effects on the matrix/particle metallurgy of the composite.

2. BACKGROUND

2.1 History and Nature of the Problem

The U.S. Army and Air Force currently utilize kinetic energy (KE) penetrators of depleted uranium (DU) alloys, principally DU-¾Ti, to penetrate the armor on threat vehicles, e.g. main battle tanks and armored personnel carriers (APCs). These penetrators range in size from those used in the Abrams tank main gun (105 or 120 mm) to the medium-caliber (25 and 30 mm) guns of the M-2 Bradley APC, the AH-64 Apache attack helicopter, and the A-10 Thunderbolt close air support aircraft. The Army has invested heavily in improved tungsten composite materials to replace DU alloys, but none has yet demonstrated performance equivalent to that of DU. Many interesting tungsten materials having different quasistatic physical properties have been developed through detailed metallurgical (thermal/mechanical/chemical) processing. However, the ballistic properties of such materials are completely predictable in 0° impact on semi-infinite rolled homogeneous armor (RHA) targets, based on tungsten content alone (which establishes mass and thus kinetic energy).

In ballistic test data for DU and some tungsten composites, including data obtained using the quarter-scale rods produced in this program (described more fully below), the tungsten content of a penetrator impacting at 0° obliquity was observed to compensate for (conceal) certain types and amounts of defects present in the penetrator [1]. This result has almost certainly been experienced during the present project, as described subsequently.

These results are all the more disappointing as the need for a DU replacement continues to grow. A significant portion of the cleanup costs for the Persian Gulf War is due to disposal of the DU-destroyed and -contaminated vehicles and equipment that litter the desert. Although there is much reticence to publicize these costs, at least one source within the government has estimated the DU cleanup bill to be on the order of $500 million-1 billion. Awareness has also been raised concerning the significant health risks and decontamination costs associated with the manufacture and handling of DU within the U.S. These costs, which are both real (dollars) and political (as the U.S. Navy experienced in the early 1980s), will continue to mount.

The Navy concluded previously that complaints about the shipboard storage of DU rounds for the 20-mm Phalanx close-in weapon system (CIWS) were intolerable, and proceeded to unilaterally develop a W:5%Ni/Fe penetrator that performed equally well against the threat target. The Navy threat target, however, is quite different from those of interest to the Army and Air Force, which are still defeated more successfully by DU penetrators than by tungsten composite materials of any type.

As noted, the Army has invested significant resources toward developing improved tungsten composites. Work both within the Army, at the Ballistics Research Laboratory (BRL), Army Materials Technology Laboratory (AMTL), Armament Research, Development, & Engineering Center (ARDEC), and Army Research Office (ARO), and in the commercial sector (GTE/Sylvania, Teledyne) has long been based on the premise that it is only necessary to improve the quasistatic mechanical properties of W:Ni/Fe composites in order to improve ballistic properties. This is an attractive rationale when considering that one type of target is a series

of two or more spaced steel plates (found on trucks, APCs, and some tanks) that impart high bending loads to the penetrator. The problem with this rationale is that it does not take into account strain rate effects. It also ignores the total, very complex stress state encountered during penetration of the most simple spaced plate target or the complex, highly oblique material combinations found in the frontal and turret armors of main battle tanks.

Improvement of low strain rate properties has not resulted in any discernable improvement in ballistic properties [2-4]. Furthermore, penetrators having tungsten contents from 90 to 95 wt% all perform similarly in zero-degree impact onto RHA semi-infinite plates when launched at velocities resulting in similar kinetic energies, and those with 97 wt% tungsten seem to perform slightly better [3]. Interestingly, in these composites increased density (more tungsten) seems to compensate for slightly poorer mechanical properties [3].

The Army Research Office funded a multiyear effort in the 1980s directed at the development of improved tungsten composites. Many metallurgical parameters and their effects on properties were investigated with regard to tungsten powder (W_p) composites, including alloying for grain refinement, impurity effects, cold and warm working, process parameter variations in the LPS cycle, post-processing heat treatment, and matrix composition variations at constant tungsten content [5]. Many of these investigations led to improved mechanical properties, such as strength and elongation; however, the goal was to improve the quasistatic properties of tungsten composites. Much optimism was expressed about improvements for ordnance applications, but none of the ARO programs studied ballistic performance as related to or affected by the metallurgical and mechanical properties being considered.

The Army Materials Technology Laboratory has conducted an extensive effort to improve the properties of W_p composites and perform ballistic testing on commercially developed materials [3,6-10]. Efforts at other Army facilities (e.g. BRL, ARDEC) have been ancillary to the AMTL efforts, in the area of materials development and characterization of physical properties.

Work at BRL produced some interesting observations regarding ballistically tested materials. The ballistic performance of several tungsten composites was evaluated with regard to mechanical properties, with only density (tungsten content) appearing to influence performance [11]. In another study, rods of pure single-crystal tungsten having orientations (presumably parallel to the penetrator axis) of [100], [110], and [111] were shown to perform differently [12]. The [100] tungsten gave the best performance, equivalent to that of DU, against RHA finite and semi-infinite plates. In explaining these observations, the [100] tungsten was said to have deformed by "favorable slip/cleavage" with "final shear localization at a favorable angle for easy material flow away from the penetration interface." In other words, the [100] tungsten performed more like a DU penetrator than a tungsten composite.

In support of these observations, DU penetration into semi-infinite RHA targets was shown to be characterized by a localized (adiabatic) shear deformation mode that permits the penetrator to discard deformed material quickly along its flanks as penetration proceeds [2]. This process leads to a "self-sharpening" effect that keeps the interface stress on the armor higher for a longer period of time. Such deformation contrasts with observations of a tungsten composite penetrator that deforms by "mushrooming" at the nose, thereby spreading the impact force and

lowering the interface stress, and permitting the armor to stop the penetrator sooner [2].

It may be concluded from the BRL work that efforts aimed at improving the quasistatic properties of W_p composites simply permit the material to hold together longer while contributing to the mushrooming problem. As a result, no net gain in penetration capability is observed in ballistic testing.

Overseas work has focused on understanding the performance of W_p composites, largely because other governments do not produce and will not purchase DU KE rounds. One study investigated and compared the post-test microstructural details of three types of penetrators: pure tungsten, tool steel, and a tungsten "heavy metal" [13]. This work noted the presence of what was termed "molten films" and adiabatic shear deformation, and observed resolidified W-Fe alloys (T_m ≈1650°C or 3000°F) adjacent to the residual tungsten penetrator and extensive shear banding in the steel penetrator. The heavy metal penetrator (W:5%Ni:3%Fe) showed regions of large plastic deformation in which the tungsten particles themselves were heavily deformed. Resolidified zones, similar to those found next to the pure tungsten penetrator, were found adjacent to the heavy metal penetrator.

Metallurgical and forging studies have been performed on W_p composites in Korea [14,15], while work in Sweden investigated the deformation behavior of high-density tungsten alloys at different temperatures from -100 to +100°C (-150 to +210°F) with regard to explaining the observed texture, grain deformation, and dislocation density [16]. A German study investigated the elevated strain rate properties of various tungsten "sinter alloys" with the goal of describing their deformation modes and behavior [17,18].

Much work has also been directed at improved W_p composite materials in Israel [19]. Powder metallurgy (PM) techniques were investigated for improving both KE penetrator and shaped charge (SC) liner materials. This work noted that most KE and SC designs use penetration behavior models that ignore the dynamic (elevated strain rate) properties of both armor and penetrator materials, and performed metallurgical studies on tungsten composites including combinations of swaging and heat treatment to optimize strength and ductility at higher tungsten contents. An improved PM tungsten-copper shaped charge liner material was also investigated.

2.2 Phase I Results and Phase II Goals

The primary objective of the Phase I program was to demonstrate a practical process for applying nickel and iron coatings to individual tungsten particles [20]. A "tumbling powder" reactor and two versions of a fluidized-bed reactor were used, and several precursors were investigated. Coatings of nickel and iron were obtained on tungsten particles (5-μm average size) in both the tumbler and the fluidized bed, although the latter promoted more complete coverage. Specimens sintered to full density at AMTL and to ≈90% density at Ultramet (due to unoptimized uniaxial cold pressing and LPS parameters) confirmed the presence of completely matrix-coated particles. Agglomerates present in the as-received commercially supplied powder were coated as such; however, the CVD coating process was so efficient that the nickel or iron penetrated the spaces between individual agglomerated particles.

The motivation for both the Phase I and Phase II studies derived from the weight of experience in mixing and sintering metal powders, as described in much of the existing W_p composite literature. The literature sources are consistent in detailing various deleterious effects resulting from the classical powder-mixing/ LPS processing route for these materials [5,21]. An excellent review of effects tending to reduce ductility in W_p composites is available [21], while the problems arising from tungsten-tungsten particle contiguity and small amounts of residual porosity are detailed [5,22]. Indeed, only ≈1% porosity results in zero elongation in 94-97 wt% W_p materials [21,22]. Embrittlement is caused by any of several factors [21]:

- incomplete oxide reduction
- residual porosity
- hydrogen embrittlement
- impurity segregation
- high tungsten content and/or surface notches
- tungsten precipitation in the matrix
- mechanical working and annealing

Ultramet's powder coating work has been based on the premise that tungsten contiguity as an embrittling mechanism can be eliminated, at least in the green shape stage of processing, by coating each individual tungsten particle with the desired matrix content. It was also believed that this benefit would continue through consolidation by LPS or HIP. A perfectly distributed matrix should reduce consolidation time with respect to blended powder materials because the matrix phase would not have to penetrate powder agglomerates or redistribute from areas of local inhomogeneity. This, in turn, would reduce the time during which rapid grain growth takes place in the liquid phase during typical LPS consolidation.

One of the advantages of fluidized-bed processing is chemical and thermal uniformity during operation. Surface oxygen contamination in the tungsten powder was reduced in hydrogen before introducing the reactant gas flows to begin matrix deposition. This procedure is believed to have been effective, and this portion of the CVD process could be further developed by increasing the reduction temperature to as high as 1000°C (1830°F), as has been done in LPS [23]. The hydrogen reduction temperature should not be raised above 1000°C, however, because the solubility of hydrogen in tungsten eventually leads to embrittlement [21]. At the very least, another processing step, such as an argon or vacuum anneal, may become necessary [24].

Efficient processing of a perfectly homogeneous W_p composite should, at least in higher tungsten content materials, minimize porosity due to problems of matrix redistribution from inhomogeneously mixed materials and penetration of contiguous tungsten grain agglomerates.

A 94 wt% tungsten material was selected based on the speculation that solving contiguity problems and eliminating grain growth would result in a significant, easily demonstrated increase in strength, impact energy absorption, and ductility. The 94 wt% range seems to be where mechanical properties drop off significantly in LPS materials, as illustrated in the mechanical properties of composites of various tungsten contents having different Ni:Fe ratios in both unworked and swaged conditions [4].

The goals of the Phase II program were to optimize the fluidized-bed CVD process developed in Phase I in order to successfully coat individual tungsten particles (5- to 20-μm) with a Ni/Fe or a Ni/Co matrix while limiting carbon and oxygen contents to less than 50 ppm and 100 ppm, respectively. The powder would then be fabricated into solid shapes large enough to obtain mechanical and ballistic test specimens (quarter-scale rods). In addition, reactor capacity was to be scaled up from 100-200 g to 5 kg and a design/economic analysis provided for a 20-kg reactor.

3. EXPERIMENTAL APPROACH

In this program, Ultramet developed a fluidized-bed CVD process capable of uniformly coating individual tungsten powder particles with nickel, iron, and cobalt for the purpose of improving the ductility and toughness of tungsten-heavy alloys. Low-temperature (relative to liquid-phase sintering) consolidation techniques were investigated in order to preserve perfect matrix distribution in the consolidated part and thereby prevent embrittlement due to tungsten-tungsten particle contiguity.

3.1 Chemical Vapor Deposition (CVD)

CVD is a coating method that utilizes the decomposition of a gaseous precursor, flowed over or through a heated substrate, with subsequent condensation from the vapor state to form a solid deposit. The CVD process is an extremely versatile and relatively inexpensive method of coating a complex shape or, in some cases, of depositing a structural part. Its benefits include the potential to produce deposits of controlled density, thickness, and composition, with extremely low impurity levels for a variety of applications [25].

The CVD process itself promotes greater purity, particularly for powder coating, as in situ gettering of contaminants can be performed in order to purify both the as-received (uncoated) powder and the resultant coatings. Also, the ability of CVD to produce multilayered or alloyed coatings allows for precise control of the desired physical and chemical characteristics of the final fabricated specimen [25].

Successful CVD depends on experimentally determining the optimal deposition parameters. These parameters include the gaseous compound of the material to be deposited, substrate temperature, gas concentration, flow, pressure and geometry within the reaction chamber, coating thickness, and substrate material. For the coating to have high integrity and adhesion to the substrate, the substrate either must have a similar thermal expansion coefficient to that of the deposited material, or form a strong chemical or metallurgical bond with it. The thinner the coating, the less similar the expansion coefficients need be. Where coating and substrate form no bond and have widely differing expansion coefficients, a good bond can often be achieved by using a thin interlayer of a third material [25].

The essential requirements of a CVD facility are that the substrate be maintained at the correct temperature and that the plating gases be supplied in the correct ratio and at the correct pressure. The substrate is typically heated resistively, inductively, or in a hot wall furnace. The composition of the plating gases is determined by the type of reaction to be used. The same material may be deposited using different compounds and different reactions at different temperatures, with each producing good coatings but different crystal structures. Compounds and alloys can be deposited by simultaneous codeposition of the appropriate elements. Some of the plating gases are volatile liquids or solids that are commercially available. In other cases, the compounds are made in situ immediately before entering the CVD chamber to produce the desired coating reaction [25].

3.2 Fluidized-Bed CVD

In order to uniformly coat fine particulates, fluidized-bed technology was investigated with the established CVD processes. The fluidized bed acts to suspend individual particles within a gas stream, where they can be coated. The gas velocity entering the fluidization zone must be greater than the terminal velocity of the particles so that particles do not settle at the bottom of the reactor, while the gas velocity elsewhere must be less than the terminal velocity of the particles so that they are not blown out of the reactor. In order to fluidize the particles, the gas velocity must be greater than the minimum fluidization velocity, u_{mf}, which is given by

$$u_{mf} = \frac{d_p^2(\rho_s-\rho_g)g}{1650\mu} \quad (\text{for } \frac{du_o\rho_g}{\mu} < 20) \tag{1}$$

where d_p is the particle diameter, ρ_s is the density of solids, ρ_g is the fluidizing gas density, g is the acceleration of gravity, μ is the gas viscosity, and u_o is the superficial gas velocity [26].

The CVD fluidized-bed coating process and apparatus developed in this program are capable of both fluidizing and coating metallic and ceramic particles as small as 5 μm in diameter with a large number of different metal and ceramic materials (see Table I).

In fluidized-bed CVD powder coating, powder particles are coated free of agglomeration, while the concentration and thickness of the deposited coating can be controlled. Standard powder metallurgy techniques involving powder mixing, pressing, and sintering may result in elemental heterogeneity and even porosity due to local segregation of tungsten and matrix powders. The use of prealloyed (uncoated) matrix powder particles eliminates the problem of matrix alloy elemental heterogeneity. Local segregation of tungsten particles, however, cannot be eliminated during LPS consolidation, especially at tungsten contents of 93-95 wt% during mixing.

The tungsten powder material utilized for this program was procured from GTE Products Corp. (Towanda, PA). Several batches of powder were purchased over the course of the program, with a typical specification sheet for the M-68 deagglomerated tungsten powder shown in Table II. The milling process utilized spherical WC-Co-Ni media in a WC-lined mill for several hours. The manufacturer's chemical analysis of the powder before and after milling indicated that the milling process increased oxygen, iron, nickel, and chromium contents in the powder; carbon and cobalt contents were not measured. The ≈12-μm tungsten powder was chosen for study because this particle size could be easily fluidized, thus reducing powder loss through the exhaust, and because the manufacturer considered this material to have minimal agglomeration.

3.3 Coating Materials

Nickel, iron, and cobalt were chosen as the matrix elements for Phase II W_p composites. Heavy metal applications require that a minimum amount of low-density matrix material be used, consistent with mechanical property requirements such as strength and ductility. As the volume fraction of the matrix is reduced, however, tungsten-tungsten particle contiguity becomes a greater problem.

Deposition at the optimal temperature leads to complete decomposition of the precursor contacting the tungsten particles. Proprietary deposition parameters were established that allowed for the simultaneous deposition of Ni/Fe or Ni/Co, which behaved similarly. These processes are also economically attractive due to their high efficiency (defined as the ratio of metal deposited to metal reacted), which varies from 70-90%.

As noted, cobalt was eliminated from the matrix of compositions to be examined due to the high cost of its precursor in small experimental quantities. The matrix of coated powder compositions to be investigated included the following:

- 90% W:10% matrix metal coating (Ni:Fe 70:30)
- 95:5 (Ni:Fe 70:30)
- 90:10 (pure Ni)
- 95:5 (pure Ni)
- 90:10 (Ni:Fe 90:10)
- 95:5 (Ni:Fe 90:10)

Due to time and budgetary constraints, however, the program was subsequently redirected to investigate only a 94:6 (Ni:Fe 70:30) composition. This material, which was the first composition investigated and from which good results and properties were obtained from the start, provided a representative comparison of properties with commercially available materials. The 94:6 composition does possess less ductility than 90:10 (Ni:Fe 70:30) material when fabricated by conventional liquid-phase sintering [4].

3.4 Impurity Minimization

One advantage of CVD is the ability to control the chemistry of the deposit by controlling that of the precursor materials [25]. In addition, purification reactions can be created at the substrate surface, such as the removal of surface oxides by hydrogen reduction. Control of the impurity level in the CVD process itself can be accomplished through the choice of metal precursor and gettering of existing contaminants. The precursors of nickel, iron, and cobalt were chosen in order to minimize contamination from reaction products.

The level and distribution of impurities, particularly carbon and oxygen, have a substantial effect on the mechanical properties of W_p composites [21]. Tungsten powder is difficult to keep oxide-free when exposed to air during handling and processing. It also lacks solubility for interstitial contaminants, which tend to segregate at grain boundaries, causing poor intergranular cohesive strength.

Ultramet showed that light-element impurity levels (especially carbon and oxygen) in tungsten powder may be substantially reduced through heat treatment, including hydrogen reduction of the as-received tungsten powder. As described below, carbon and oxygen levels were reduced by 60%. Many other researchers have noted the importance of reducing the carbon and oxygen contents of tungsten-heavy metal composites in order to maximize mechanical properties [5,21].

Incorporation of light-element impurities during the manufacturing and deagglomeration of tungsten powder is inevitable. Prior to being coated, the as-received powder was reduced in hydrogen at a temperature that is high enough to promote reduction yet low enough to avoid appreciable contamination of the

tungsten by the hydrogen [21]. A post-coating hydrogen reduction was also conducted to remove any impurities incorporated in the coating, prior to consolidation. Table III shows the effect of hydrogen reduction on the levels of oxygen and carbon in as-received 5- and 20-μm tungsten powder. The concentration of the primary embrittling contaminant, oxygen, is reduced to less than one-third its original value, while the already low level of carbon is reduced even further.

3.5 Uncoated and Coated Powder Characterization

Uncoated (as-received) and coated powders were characterized both in-house and externally. In-house analysis included evaluation of coating uniformity and degree of powder agglomeration by scanning electron microscopy (SEM). Energy-dispersive X-ray (EDX) microanalysis was utilized to determine the presence and distribution of the composite elements, although it was determined that accurate quantitative analysis could not be achieved by this method. Precise analysis of the metal and light element constituents of the coated powder material was performed by Teledyne Wah Chang (Albany, OR). The procedures, reporting limits, and precision limits for the chemical analysis are shown in Table IV.

Figure 1 shows SEM micrographs of as-received 12-μm tungsten powder. This powder material was optimal for this study due to its relatively narrow particle size distribution and lack of sharp edges and agglomeration. Figure 2 shows SEM micrographs of coated 12-μm tungsten powder. The backscattered electron image (BEI) segment of Figure 2A (at bottom) shows little contrast in W:4.3%Ni:1.7%Fe powder, signifying a uniform coating. The BEI segment of Figure 2B, by comparison, shows an example of the extreme contrast noted in many (initially) nonuniformly coated powder batches, due to the large difference between the atomic numbers of tungsten and nickel/iron. The secondary electron images (SEI, at top) show surface morphology, as opposed to the elemental differences emphasized by BEI. Figure 3 is a SEM micrograph of a coated W:4.3%Ni:1.7%Fe grain surface at high magnification. The coating is composed of a multitude of fine nodules that nucleated at the particle surface and combined to form a dense coating. This morphology is typically of thin (micron-level) coatings, which form local nucleation sites that grow laterally as well as outward.

3.6 Powder Consolidation Techniques

Three consolidation processes were investigated in this work: liquid-phase sintering (LPS), hot isostatic pressing (HIP), and a unique derivative of HIP involving dynamic force. The latter two induce compaction by both mechanical force and solid-state sintering. Each of these methods has both positive and negative aspects with regard to ease of compaction, degree of densification, and the level of impurities added to or removed from the material. The W_p composites of interest herein provide a challenge to any consolidation technique due to the large volume of stiff (E $\approx$420 GPa or 60 Msi), high-compressive strength ($\sigma_{y(compression)}$ $\approx$4.5 GPa or 650 ksi) particles.

3.6.1 Liquid-Phase Sintering (LPS)

Liquid-phase sintering utilizes a liquid phase to enhance diffusion and reactivity during the sintering step. LPS drastically reduces the times and

temperatures required to achieve complete densification in high melting point systems such as tungsten composites. The powders to be sintered are first compacted by cold isostatic pressing (CIP) to form the green body. Pressures ranging from 140 to 310 MPa (20-45 ksi) are typically used, depending on the powder size and shape. Isostatic pressing is used for high length-to-density ratio (L/D) compacts such as penetrator shapes because the frictional forces of the powder, particularly against a steel die wall, lead to pressure gradients and result in a variation of density within the piece. During sintering, these density variations must be overcome by material flow, resulting in warping, variable shrinkage, and a loss of the original tolerances. The sintering cycle itself usually involves a complex time-temperature cycle composed of binder burnout (if binder is used), oxide reduction in hydrogen, a sintering step, controlled cooling, and finally a hydrogen diffusion anneal. A sintering cycle must be designed to give complete limiting grain growth for each matrix composition, shape, size, furnace, etc.

Even though ball-milled powder mixtures can produce a range of particle sizes that can be pressed/sintered to an acceptable density, Ultramet's monosized coated tungsten powders did not sinter well. The sintering behavior of the Ultramet material was studied after it was first characterized for chemistry and particle size distribution [27]. Three lots of powder were obtained, all coated with Ni/Fe but having different total matrix contents ranging from 1 to 4 wt%. The higher matrix content material gave higher sintered densities than did lower matrix contents, but in no case higher than 90% of theoretical. Coated tungsten particle size was 18.44 μm on average, with 73 wt% of the sample being <22 μm. The narrow particle size distribution was shown to be the primary limiting factor on sinterability. After mixing 20% wt% of tungsten, nickel, and iron powders having particle sizes $\leq$1 μm (while maintaining proper W:Ni/Fe compositions) with the Ultramet powder, a sintered density of 93% was obtained. This result indicated that adjusting the particle size distribution would likely improve the densities achieved substantially.

The optimal particle size distribution can be estimated using several "cuts" of different sized particles. The proper size distribution can then be calculated based on the assumption of random, close-packed particles with successive particle sizes calculated to fill the interstices between larger particles. When two particle sizes are used, optimal packing densities are normally achieved when the ratio of coarse to fine particles is approximately 70:30.

3.6.2 Hot Isostatic Pressing (HIP)

To obtain high density together with fine particle size, particularly for materials such as tungsten, the combination of isostatic pressure and high temperature is an effective densification technique for PM shapes, even those that are relatively complex. One of the main advantages of HIP is that material preparation is less critical than with LPS processes. Because isostatic pressure and heat are applied simultaneously, material flow and rearrangement can take place in the solid state. Reduced processing temperatures can be utilized, thus reducing the amount of grain growth and particle coarsening that occur in W_p composites. The HIP technique involves placing the powder to be compacted in a steel can, which is then sealed by electron beam welding under vacuum, followed by the application of heat and pressure (using an inert gas) in a water-cooled autoclave.

3.6.3 Ceracon®

The primary difficulties associated with HIP, which include the relatively long processing time and the inconvenience and expense associated with the "canning" of the powder preform, can potentially be overcome using the patented Ceracon process. The Ceracon process is designed to be a low-cost powder consolidation process for achieving near-net shape, full-density parts, utilizing conventional powder metallurgy equipment and setup. The Ceracon process is a quasi-isostatic, hot consolidation technique that substitutes a ceramic particulate material as the pressure-transmitting medium for the inert gas used in HIP. Pressures to 1450 MPa (210 ksi) can be used, as compared to 275 MPa (40 ksi) for HIP, and materials can be processed using temperatures up to 1800°C (3270°F). The Ceracon process is illustrated schematically in Figure 4.

In the first step of the Ceracon process, a simple die is heated and filled with the pressure-transmitting medium (PTM), which is preheated to 50°C (90°F) above the preform consolidation temperature. The preform may have a green density of up to 80% and can be fabricated by conventional techniques such as cold pressing, CIP, etc. The heated preform is then lowered into the die, which is partially filled with the hot PTM. After the preform is embedded in the PTM, a hydraulic press is lowered onto the PTM (which now surrounds the part) and sufficient pressure is applied to consolidate the preform to full density.

The Ceracon process may be much more versatile than HIP because the rate of pressure application is limited only by the hydraulic press used, and the peak pressure is limited only by the die enclosure for the PTM, the press capacity, and the properties of the PTM itself. Improved properties may be achievable with the Ceracon process due to the higher pressures and pressure application rates used, as well as the shorter processing times required.

The amount of time a sample is subjected to Ceracon consolidation is significantly shorter than the one to six hours needed for uniaxial hot pressing or HIP processes. Particle coarsening is significantly reduced, and tungsten dissolution in the matrix is reduced or eliminated. The Ceracon process could provide the benefits of isostatic pressing while drastically reducing consolidation times.

Potential problems may occur due to the properties (limitations) of the PTM. Temperature and pressure gradients could exist due to the quasi-isostatic nature of the pressure transmission. Scale-up of process parameters for increased quantity, size, and complexity of parts must be done cautiously. Finally, the fast consolidation may be both advantageous and disadvantageous, depending on the requirements of the metallurgy of the system being fabricated. For example, with W_p composites, some dissolution of the tungsten in the Ni/Fe matrix may be necessary. Post-consolidation heat treatments may be applicable in any case.

3.7 Mechanical Testing

3.7.1 Flexure and Compression Testing

In order to evaluate the strength and ductility of Ultramet-coated powder/ Ceracon-consolidated composites, three-point flexure testing was performed at Ultramet and compressive Hopkinson bar testing was conducted at the University

of California, San Diego (UCSD). The latter was exploratory in nature, with only four specimens deformed.

Three-point flexure testing was chosen to evaluate both strength and ductility by measuring maximum flexural stress and midspan deflection. Specimen dimensions were limited by the consolidated billet size available; therefore, the data shown should be used only to draw general conclusions about the various materials tested. It is important to note that these data were obtained using the smaller (1" diameter x 1" long) billets described above.

Flexure test specimens were fabricated using an aluminum oxide cutoff wheel on a surface grinder. The wheel thickness was 0.020", with the workpiece flooded with coolant. RMS surface roughness following cutting was 0.016". All edges were polished with an aluminum oxide deburring wheel to a radius of 0.010". Visual inspection at 30-100x showed no chips or cracks on the edges.

The three-point loading scheme, shown in Figure 5, was performed in-house using an Instron model 1122 mechanical tester. Proper alignment of the flexure bars is ensured by the use of a flexible metal tab that is attached to the lower supports, perpendicular to their length. The specimens were tested at ambient temperature using a cross-head speed of 0.010"/min.

Compressive Hopkinson bar specimens (0.150-0.200" diameter x 0.156" long) were fabricated in a similar manner to the flexure specimens, with the dimensions varying according to the size of the billet available. The compositions of these specimens were 94.9W:3.8Ni:1.3Fe and 95.3W:3.5Ni:1.2Fe.

3.7.2 Tensile and Charpy Impact Testing

Large billets (3.25" x 0.9" x 0.7") of 94 wt% (nominal) W_p material, consolidated by Ceracon, were furnished to AMTL for fabrication into un-notched Charpy specimens for tensile and impact testing, and quarter-scale long rods for ballistic testing. The tensile and Charpy specimens (types TR-6 and CV-12, respectively) are shown schematically in Figures 6 and 7. Details of the fabrication procedures were not made available, but can be described as state-of-the-art. The ballistic specimens are described below.

3.8 Ballistic Testing

Ten 0.238" diameter x 2.38" long (L/D = 10) penetrators and nine 0.307" diameter x 3.065" long (L/D = 10) penetrators were furnished to AMTL. The latter group of nine penetrators was subsequently delivered to Alliant Techsystems (Brooklyn Park, MN) for ballistic testing. Penetrator blanks were cut by electro-discharge machining (EDM) from Ceracon-consolidated billets of dimensions 3.25" x 0.9" x 0.7", with finish machining by lathe. Seven of the nine rods were tested at Alliant, with five fired into a spaced array target of two plates leaning against each other in "tepee" fashion and two fired into oblique, semi-infinite armor steel blocks for a depth-of-penetration test. The plate and block dimensions and complete target descriptions are proprietary to Alliant. The two untested penetrators remain at Alliant for elevated strain rate testing.

Flash radiographs were taken before impact, between the plates, and after the penetration of the second of the spaced array plates. The gun was warmed up with

preliminary shots using Teledyne W:7%Ni/Fe LPS rods so that velocities were properly repeatable. Orthogonal X-ray exposures determined pitch and yaw to the nearest degree just before impact on the solid steel block and on the first inclined plate. Seven impacts were acceptable for pitch and yaw (the criterion was a maximum deviation of 1° in each direction), and the other two were marginally acceptable.

Velocity ranges were 3111-3130 ft/sec for the two penetrators into the semi-infinite monoblock targets and 5183-5265 ft/sec for the five penetrators into the spaced array targets. All targets are preserved in archive storage, as well as the penetrator fragments found in soft capture packs of paperboard behind the spaced array targets. The two monoblock targets (presumably containing residual penetrators) were retained at Alliant. Penetrator weights, actual pitch/yaw data, velocity data, residual penetrator fragment data, etc. are available from Alliant.

4. RESULTS AND DISCUSSION

4.1 Consolidated Powder Evaluation

Metallography was performed in-house on consolidated billet cross-sections, using SEM and EDX analysis to determine the structure and uniformity of the composite material. It should be noted that the following analysis of billet cross-sections includes various compositions, with each composition representing the powder material that was available at the time of the particular consolidation study. In the case of LPS, a commercial W:10%Ni/Fe material was evaluated, as difficulty in achieving full density with Ultramet's monosized powders precluded the use of LPS for consolidating billets for mechanical and ballistic test specimens [27]. Ultramet-coated W:5% matrix material was used in the HIP study, while the Ceracon study employed an Ultramet-coated W:5-6% matrix composition.

The addition of uncoated 5-μm tungsten powder was investigated with both the Ceracon and HIP processes, with the intent of producing a slightly better particle size distribution and possibly improving the density of the consolidated material [27]. Prior to fabrication of the deliverable ballistic penetrator material, however, it was decided that this practice could complicate the analysis of performance and failure modes, so no uncoated tungsten powder was added to the penetrator material.

4.1.1 LPS-Consolidated Material

Figure 8 is a SEM micrograph of a typical commercial W:7%Ni:3%Fe composite that was consolidated by LPS. Extensive areas of nonuniform matrix distribution are evident, along with tungsten-tungsten particle contact, which promotes crack formation and propagation leading to brittle behavior. This program was directed at producing a more uniformly dispersed matrix via CVD fluidized-bed processing, and evaluating the resultant changes in mechanical and ballistic performance.

4.1.2 HIP-Consolidated Material

HIP consolidation was performed at IMT (Portland, OR) at temperatures ranging from 400-1400°C (750-2550°F) and pressures of 80-200 MPa (12-30 ksi) over processing times of 1-4 hours. The coated powder material was first loaded into stainless steel containers, 1" diameter x 1" long, which were sealed by electron-beam welding under vacuum. In order to minimize time and expense, the Ultramet billets were consolidated during IMT-standard HIP cycles being performed on nickel aircraft parts, with optimization of parameters for the Ultramet material expected to be performed later, but resources were not available for this work.

Figure 9 is a SEM micrograph of a W:3.5%Ni:1.2%Fe composite consolidated by HIP. Noticeable segregation of the Ni/Fe matrix to the void spaces between the tungsten grains occurred, resulting in tungsten-tungsten particle contact. Figure 10 shows an EDX line scan and elemental map of a HIP-consolidated W:3.5%Ni:1.2%Fe composite. The nonuniformity of matrix distribution is evident in each case.

Virtually all of the specimens consolidated by HIP exhibited this microstructure. The specimens consolidated at lower temperatures could not be evaluated in cross-section due to a lack of structural integrity. Increasing the temperature,

pressure, and process time for HIP had little effect on the microstructure even though the density increased. Although full theoretical density (18.24 g/cm^3) was eventually achieved, the scope of this study did not allow for a detailed evaluation of various combinations of material compositions and process conditions. It is felt that an optimized HIP cycle, perhaps with a programmed (slower) application of pressure and a lower temperature, would produce an excellent microstructure having full density and no matrix segregation or W_p grain growth.

4.1.3 Ceracon-Consolidated Material

For evaluation of the Ceracon process, consolidation temperatures of 1000-1500°C (1830-2730°F), pressures of 1000-1500 MPa (145-220 ksi), and process times of 10 to 120 seconds were investigated. Figure 11 shows SEM micrographs of typical microstructures from small (1" diameter x 1" long) billets consolidated at lower temperatures. The uniformity of matrix distribution, as evidenced by the coating surrounding each tungsten grain, is clearly seen. Figure 12 shows SEM micrographs of a W:3.5%Ni:1.5%Fe microstructure taken from the outer surface of a billet to its center. The exterior surface of the billet, ≈0.050" deep, contained a degree of porosity that could be machined off, leaving virtually pore-free material. The surface porosity resulted from the fact that as the part is transferred from the furnace to the die, the outer surface cools, thereby decreasing particle mobility while under pressure. In order to prevent this phenomenon, the temperature of the PTM may need to be higher than the normal 50°C (90°F) above the processing temperature. Waiting 1-2 minutes for the part to re-equilibrate after being surrounded by the PTM may also be beneficial.

Achieving full density in larger (3.25" x 0.9" x 0.7") billets of W:4.3%Ni:1.7%Fe material required higher temperatures. This larger billet size was required to fabricate quarter-scale ballistic test specimens. As discussed below, the optimal combination of strength and ductility was achieved in material that underwent a "quasi-optimized" Ceracon consolidation using proprietary process conditions. The higher temperature processing seemed to result in greater tungsten-tungsten particle contact, as seen in Figure 13A, though some degree of coating can be seen on nearly all the tungsten grains at higher magnification (Figure 13B). An EDX line scan across the matrix, shown in Figure 14, indicates strong peaks for nickel and iron, with little or no dissolved tungsten in the matrix. The short consolidation times involved in the Ceracon process effectively eliminate matrix dissolution of tungsten. The effects on mechanical properties of little or no dissolved tungsten in the matrix, as compared to that in state-of-the-art W_p composites, were not addressed in this study, but definitely warrant future investigation.

4.2 Mechanical Testing

4.2.1 Flexure and Compression Testing

Table V shows the results of flexural testing of HIP specimens fabricated at IMT. As noted above, HIP processing was not optimized and microstructures showed extensive tungsten-tungsten particle contact as well as pooling of the matrix (see Figures 9 and 10), as if it had been extruded from its initial homogeneous distribution by excessive time under pressure. The addition of extra tungsten to subsequent billets may have hindered matrix redistribution, resulting in

higher relative density and better strength and elongation in spite of an essentially unacceptable microstructure. In any case, fabrication resources were concentrated on the Ceracon process, even though the HIP process could have been optimized to eliminate the poor microstructure.

Thirteen W:4.3%Ni:1.7%Fe billets were consolidated by the "quasi-optimized" Ceracon process, and were then used for Charpy and tensile specimens (three billets) and ballistic specimens (ten billets). The flexural data obtained from Ultramet/Ceracon specimens are presented in Table VI. The rightmost column of Table VI represents the data obtained from the first quasi-optimized consolidated billet. Only one of these specimens was broken because the rest of the material was delivered to AMTL. The midspan deflection was measured to be 0.024", matching the best value achieved with any Ultramet/Ceracon material, and the maximum (fracture) stress was found to be 2100 MPa (305 ksi), which is nearly 90% of the highest fracture stress achieved to date. The data in the leftmost three columns of Table VI were obtained from relatively small billets, whereas the data in the rightmost four columns were obtained from billets of the larger size from which quarter-scale penetrators, tensile specimens, and Charpy specimens were machined.

Figure 15 is a photograph of a flexure bar, produced from the quasi-optimized consolidation material described above, which was removed from the testing rig just prior to the expected fracture in order to show the plastic deformation.

Table VII compares the fracture strength and ductility (midspan deflection) of tungsten composite material consolidated by HIP, LPS, and the Ceracon process (small billets). It should be noted that the LPS material was fabricated by conventional powder mixing from a commercial source. Ceracon consolidation is characterized by a trend toward better flexural strength and ductility (midspan deflection) with increasing density. All micrographs of Ceracon-consolidated material show the presence of matrix material around each tungsten particle, a primary goal of this work. The mechanical properties of specimens from small billets seem to be better than those of specimens from large billets, with the exception of the two specimens in the rightmost columns of Table VII, which approach the values for small billets. SEM micrographs of Ultramet/HIP, commercial/LPS, and Ultramet/Ceracon material (Figures 16-18) show comparative fracture surfaces representative of the different processes.

The Ultramet CVD/HIP material (Figure 16) exhibited an almost entirely intergranular fracture mode. The sharp-edged, faceted fracture surfaces resulted from the brittle fracture behavior that is expected at the interface of tungsten grains in direct contact. The matrix material, initially designed to provide an interface between tungsten grains, was extruded into triple point locations between grains. These high matrix content areas are clearly evident in the micrographs. In addition, a portion of the intergranular fracture most likely involved the breaking up of the several tungsten polycrystals that make up the larger tungsten grains, prior to CVD coating.

The commercial powder mixing/LPS material exhibited fracture in virtually a single plane of tungsten particles. The facets on individual tungsten grains (Figure 17A) were interfaces between tungsten particles with no matrix material present. Figure 17B clearly shows the bright tungsten-tungsten facets on individual tungsten grains, with no sign of the Ni/Fe matrix material. The result was again predominantly intergranular failure.

The Ultramet CVD/Ceracon material (Figure 18) exhibited fracture behavior that was significantly different from that of the other two materials (LPS and HIP). There was evidence of three different failure modes: intergranular, intragranular, and grain pullout. The latter was different from that shown in the HIP sample, in that the void left by the removed grain was lined with Ni/Fe matrix material. The high transverse rupture strengths and encouraging deflections of the most dense specimens are attributed to the low incidence of tungsten-tungsten particle contact.

Figures 19 and 20 show the split Hopkinson bar compression data plots produced at UCSD. All four specimens were consolidated by HIP at IMT. As seen in the data, true strains were approximately 28% for the 3900/sec and 4000/sec strain rates, and 76% for the 5000/sec strain rate. Yield strengths were all approximately 1900 to 2075 MPa (275-300 ksi); the extra uncoated tungsten powder added to specimens 200-1/3 and 300-1/3 had no observable effect on the stress-strain properties. Engineering strains were ≈22% for the lower strain rate and ≈53% for the higher strain rate, indicating the presence of some elastic recovery in these composites. All specimens were recovered intact with no spalling and little or no cracking visible at 30x. The purpose was simply to demonstrate that the specimen could be recovered from this testing and to obtain some initial stress-strain data at elevated strain rates in the ballistic regime.

4.2.2 Tensile and Charpy Impact Testing

Five tensile specimens were broken from two billets consolidated by the quasi-optimized Ceracon process, using a crosshead speed of 0.01"/min. The performance of all five specimens was reasonably consistent. Ultimate tensile strengths were also consistent, even though three of the five specimens broke outside the gauge length, including one that broke in a threaded region.

Elastic moduli were approximately 290 GPa (42 Msi) for two of the specimens. The elongations of these specimens were less than 1%, while those of the other three were not measured. As a result, only fracture strength data are available for all five specimens. Ultimate tensile strengths ranged from 1000-1050 MPa (145-150 ksi). Figure 21 shows typical load elongation data obtained at AMTL.

From the two specimens for which load/displacement data are available (see Figure 21), it appears that only limited ductility is present, with at most 1-2% elongation estimated. This essentially brittle behavior was also observed at elevated strain rates in the ballistic tests. It is believed that this behavior is due to the presence of porosity, which was observed by AMTL in ballistic test specimens in amounts of 0.5-1.0 vol% (see Figure 22). Even though porosity exists, however, the total porosity fraction is likely still far below that which can be observed with immersion (water displacement) density measurement techniques. Ultramet verified that all of the billets used for mechanical and ballistic testing had a minimum of 99.5% theoretical density, based on a chemistry of W:6% matrix material.

Six un-notched Charpy specimens were broken using a Baldwin impact tester. The results confirmed the brittle behavior of the tensile specimens, with energy absorption values ranging from 1.28 to 1.44 ft·lb. Typical LPS W:5%Ni/Fe specimens absorbed 5-10 ft·lb, as interpolated from results for 93:7 and 96:4 material [4].

4.3 Ballistic Testing

Some general conclusions may be drawn from comparing the performance of Ultramet CVD/Ceracon W:6%Ni/Fe penetrators vs. Teledyne powder mixing/LPS W:7%Ni/Fe penetrators against the same targets. Performance against oblique, semi-infinite monoblock targets cannot be evaluated at this time, because results have not yet been received from Alliant concerning any residual penetrator mass remaining in the blocks. The difference in performance against the spaced array targets was clear from comparison of flash radiographs of penetrators before, during, and after penetration of the plates. Copies of these photographs have not been provided for publication, but their general features can be described.

In making the following descriptive comparisons, it is important to remember that the LPS material was W:7% matrix and has undergone extensive commercial process development in an attempt to optimize performance vs. process procedures (heat treatments, warm and cold mechanical working, etc.). Ultramet material, conversely, has only just begun fabrication development and property measurement, and no optimization of fabrication process metallurgy has been attempted as yet. The initial objective of the Ultramet/Ceracon effort was to produce material with minimal porosity, and no time or resources remained for process development.

Qualitative observations of flash radiographs and residual penetrator fragments caught by "soft capture" indicate that the Ceracon-consolidated 94 wt% tungsten Ultramet penetrators did not have nearly the resistance to high strain rate deformation and fracture as did the LPS-consolidated 93 wt% tungsten Teledyne material. The only identifiable reason for this effect was the presence of 0.5-1.0 vol% porosity observed during optical microscopic analysis at AMTL of recovered fragments of depth-of-penetration test specimens that had been fabricated from material consolidated at Ceracon using the same process parameters as those for the Alliant ballistic test specimens.

Although the Ultramet rods penetrated both plates in all five tests, they did so with far less residual mass, which represented a higher number of much smaller fragments than that of the LPS penetrators. Investigation of the fracture surfaces of the penetrator fragments, to observe whatever porosity that may be present, would likely be informative. The fact that there could be 0.5-1.0 vol% porosity contributing to failure of either mechanical or ballistic test specimens is not inconsistent with the typical water immersion measurements of 99.5% density for individual mechanical or ballistic test specimens.

Figure 23 shows the results of depth-of-penetration ballistic tests performed at AMTL on Ultramet coated powder material. These data indicate that performance is almost entirely density-related, as opposed to reflecting mechanical properties. Figure 24 compares the Ultramet material with two other tungsten composites and DU [1]. Table VIII provides the relevant test data for the Ultramet specimens.

5. CONCLUSIONS AND RECOMMENDATIONS

5.1 Summary of Results

The primary goal of this Phase II program was achieved: a viable fluidized-bed CVD tungsten powder coating process was developed and characterized. An effective hydrogen reduction treatment was demonstrated within the fluidized bed to reduce surface oxide content on the powder prior to depositing the Ni/Fe matrix. The versatility of this technique indicated that, with further development (i.e. exploring a matrix of treatment parameters vs. tungsten particle sizes), oxide contents could be further reduced, possibly to ≤50 ppm. Such work could be part of a prototype production scaleup effort wherein coating parameters are developed for a range of tungsten particle sizes, which would solve one of the major problems encountered in this program: that most consolidation techniques cannot easily work with a monosized or very narrow powder particle size distribution. However, fluidized-bed CVD parameters were most easily developed while using narrow tungsten powder particle size distributions, namely ≈5 and ≈12 μm. These particle sizes did not change significantly with deposition of the Ni/Fe matrix. This is an issue which should receive more development attention; broader particle size distributions should be explored in fluidizing experiments so that the coated powders can be more easily incorporated into existing consolidation processes (e.g. LPS) in order that this technology could used sooner for state-of-the-art PM fabrications.

The Ultramet material that yielded such encouraging flexure data compared to concurrently tested commercial W:10%Ni/Fe LPS material could not reproduce this advantage when the Ceracon billet size was increased to accommodate fabrication of mechanical and ballistic test specimens. Most likely, the Ceracon consolidation technology simply could not be scaled up to a larger size and quantity of billets in only a limited series of experiments. Unfortunately, adequate resources were not available to iterate the Ceracon process parameters vs. mechanical properties achieved. Further, the porosity that was evident during characterization of tensile test specimens at AMTL was not found in Ultramet's characterization of flexure specimens taken from the smaller billets that had given the high modulus of rupture values and encouraging deflections compared to commercial W:10Ni/Fe LPS material.

It is likely that rapid scaleup was attempted of a process which, by nature, is not easily scaleable. The nonmetallic powder PTM is subject to pressure and thermal conductivity gradients due to the fact that powder particles comprise, at best, a quasi-isostatic medium. For instance, the particles could fracture and then densify at various locations throughout the PTM volume over many consolidation runs. Contaminants from various green parts or the various cans containing powders for consolidation could activate sintering at various locations in the PTM. Very slight non-spherical morphologies present in the original PTM could, over many high-pressure runs, develop large-scale preferred orientations, resulting in density gradients and nonuniform temperatures. The only real solution may be to remove, resize, and confirm PTM properties (particle size distribution, thermal conductivity, surface area, etc.) after almost every run, which would be a prohibitive requirement. Future experimentation on this material should include the effects of post-consolidation heat treatment and mechanical working, which have proven to be critical steps in the fabrication of state-of-the-art tungsten-heavy alloys.

Any further development of these CVD coated composite powders should include a consolidation technology that is not developmental itself, e.g. HIP. Even though HIP is perceived as a high-cost process (though half as expensive as Ceracon), it is certainly much closer to being isothermal and isostatic, and would allow much faster scale-up of part size and quantity.

Another issue arising from the drastically different mechanical properties obtained from small and large billets is the question of the optimal matrix composition and matrix-particle interface. The commercial LPS matrix material contains tungsten in solid solution, perhaps 20-30 wt% under the optimal sintering conditions and subsequent cooling/heat treatment. The importance of matrix composition, especially near tungsten particles, and its effect on the mechanical properties of the system have been noted previously [4]. Furthermore, even though CVD coating of tungsten powders is capable of restricting carbon and oxygen levels in the composite powder to <20 and <200 ppm, respectively, the spatial locations of the carbon and, more importantly, the oxygen should be investigated. A thorough surface science analysis is recommended, using secondary ion mass spectroscopy (SIMS), electron spectroscopy for chemical analysis (ESCA), electron energy loss spectroscopy (EELS), etc. to locate the oxygen and carbon and establish its chemical state (compounded, alloyed, etc.).

5.2 CVD Reactor Design

In conjunction with ongoing powder coating work at Ultramet [28-33], a new large-capacity, semicontinuous fluidized-bed CVD reactor has recently been designed and constructed, and is currently in the process of checkout and trial runs. The details of this reactor are proprietary to Ultramet, but it will offer several key advantages for powder processing. First, it can accommodate larger batches of powder in a single run. A trial run was conducted with a 5-kg batch of 12-μm tungsten powder, in order to determine the effectiveness of powder transfer. The entire charge was transferred in less than three minutes. Second, the new reactor will require significantly lower flows of both precursor gas and carrier gas, amounting to only 15% of the total flow required by the existing apparatus. Wall deposition, a common problem in conventional fluidized beds, will be reduced. Third, the new reactor is easily scaleable.

5.3 Economic Study of Coated Powders

Based upon the fluidization behavior and other knowledge gained during the course of this program, it has been determined that uniformly coating 12-μm tungsten powder particles with CVD nickel/iron in a 20-kg batch size is not feasible. However, following coating of a given powder charge in a 5-kg reactor, the coated powder can be exhausted into an external vessel, after which a new batch of uncoated powder could be introduced without terminating the run. Although the individual run capacity for such a reactor would be 5 kg, the coating process could be regarded as continuous and, therefore, the capacity considered virtually unlimited, with reactor operation halted only for maintenance. Conventional fluidized-bed reactors find their primary utility in the decomposition of the powder charge, a process that is significantly easier to scale up, as the uniformity of fluidization (gas dispersion within the powder charge) is not as critical as in the coating of powder particles.

The estimated cost for a fully operational, 5-kg batch size quartz reactor is less than $3,000. This cost is approximately five times that of the smaller, simpler reactor used during this program. Estimated instrumentation costs for production in the "research mode" are approximately $4,000, while more precise control for full-scale production would involve instrument costs ranging from $20-30,000.

Following is a tabulation of the equipment, plant, and material requirements to complete the first year of operation of a pilot coated powder production plant which Ultramet would codevelop.

* Equipment

Vacuum pumps and accessories	$ 6,000
Hoods (4)	8,000
Scrubbers (2)	10,000
5-kg fluidized-bed CVD reactors (4)	12,000
Gas supply and monitoring	4,000
Miscellaneous	2,000
Testing and quality control (metallography)	10,000
Office equipment	7,000
Equipment subtotal	$ 59,000

Note: Equipment costs are estimated from wholesale catalogs. Each reactor is estimated to produce 5 kg/shift.

* Personnel

Engineers (2)	@ $19.23/hr	$ 80,000
Shop foreman (1)	@ 14.42/hr	30,000
Technicians (4)	@ 10.58/hr	88,000
Maintenance (2)	@ 9.61/hr	40,000
Administration (1)	@ 9.61/hr	20,000
Labor subtotal		$258,000

* Plant Lease (8,000-10,000 ft^2, for one year) $ 36,000

* Legal, Patent, and Incorporation Expenses $ 10,000

Total $363,000

Note: Personnel and plant lease costs are based on average rates for the Central Plains states provided by the Merchants and Manufacturers Association (M&M) (Los Angeles, CA).

The estimated production cost of 1.0 kg of W:4%Ni:1%Fe coated powder is broken down as follows (all quoted prices are retail).

* Composition per kg coated powder:

Tungsten	950 g
Nickel	40 g
Iron	10 g

*	Raw Material Costs:		
	Tungsten powder (M-68, deagglomerated, 12.5-μm average particle size, from GTE)		$ 20.00/kg
	Nickel precursor		$ 77.78/kg
	Iron precursor		$ 25.65/kg
*	Metal Yield and Cost per kg metal:		
	Tungsten:	same as raw material	
	Nickel precursor		
	metal yield		34.4%
	cost per kg of nickel		$226.10
	Iron precursor		
	metal yield		28.5%
	cost per kg iron		$ 90.00
*	Deposition Efficiency:		
	Tungsten		90% (estimated)
	Nickel		70%
	Iron		70%
*	Material Costs per kg coated powder:		
	Tungsten	(20.00 x 0.95)/0.90 =	$21.11
	Nickel	(226.10 x 0.04)/0.70 =	$12.92
	Iron	(90.00 x 0.01)/0.70 =	$ 1.29
	Total		$35.32/kg
*	Processing Costs (based on 4 reactors, 5 kg/batch, 1 batch/day):		
	Daily production		20 kg
	Technician (2)		$10.58/hr
*	Total Labor Costs per kg coated powder:	((2 x 10.58) x 8)/20 =	$ 8.46/kg
*	Packaging, Shipping, and Clerical		$10.00/kg
	Note: Packaging, shipping, and clerical costs are based on average rates for the Central Plains states provided by M&M.		
*	Total Cost:		
	Materials		$35.32
	Labor		8.46
	Miscellaneous		10.00
*	Total Production Cost		$53.78/kg

5.4 Potential Applications

The combined new technologies developed in this work can potentially mitigate or remove the present barriers to improving powder metallurgy component fabrication. The result will be components with dependably better properties and narrower, more predictable statistical property distributions. The size and weight of load-bearing sections of components can be reduced without giving up strength,

or strength can be increased without increasing size and weight. A narrow, more predictable statistical variation in mechanical properties provides more confidence in designing structures utilizing such new materials.

In addition to the ordnance applications of interest to this program, Ultramet's powder coating technology has many more subtle, but potentially very important, benefits to both government and commercial interests. Powder metallurgy recently has made great strides in the fabrication of difficult-to-process alloys, including metastable structures for increased wear and corrosion resistance as well as stronger alloys to permit weight reduction. The latter is of great interest to many military systems, among them helicopters, fighter aircraft, ground vehicles, and artillery.

Prospects are also very good for making use of this technology in the fabrication of cemented carbide tools and wear parts, currently a $1 billion market. It is likely that these tools' transverse rupture strength and impact strength can be measurably improved. Ultimately, the entire area of metal/ceramic composites will be impacted by this technology. One example of such an advanced composite is ceramic-strengthened intermetallic materials for use in aerospace engines and structures.

While this effort has focused on the development of improved powders for tungsten heavy metal composites, this technology is being extended to develop a wide range of powder compositions for the metals, ceramics, and composites industries. Among the compositions and applications that are ready for immediate development are the following:

- Custom-coated powders for plasma spraying.

- Ceramic powders integrally coated with their corresponding sintering aids. Like the tungsten composites, this leads to reduced sintering times and temperatures, reduced grain growth, reduced contamination, and improved properties and economics.

- Matrix-coated silicon carbide (SiC), aluminum oxide (Al_2O_3), boron carbide (B_4C), cubic boron nitride (CBN), diamond, and other powders leading to improved cutting tool performance and improved plasma-sprayed wear-resistant coatings.

- Matrix- and/or interface-coated whiskers and particulates leading to injection-moldable, more cost-effective composites.

- Extension of mechanical alloying technology to include interstitial-sensitive metals such as titanium and niobium. The mating of CVD and mechanical alloying theoretically allows almost any combination of materials to be fabricated in a dispersion-strengthened composite.

- Diffusion barrier/compatibility layer coating of microspheres, powders, and particulates providing wetting and stability of fillers and reinforcements. Potential applications include stabilizing filler particle oxidation state for high temperature magnetic and electronic applications, modifying the bonding and long-term stability of SiC whiskers in titanium alloys, among others.

5.5 Acknowledgements

Ultramet would first like to acknowledge the continuous interest and support of the AMTL program monitors, Kenneth J. Tauer and Robert J. Dowding. Ultramet would also like to thank Ramas Raman and Sundeep Rele of Ceracon Inc. for their advice and assistance in the area of coated powder consolidation. Patrick Woolsey of AMTL conducted depth-of-penetration testing of Ultramet penetrators, while spaced plate testing of the penetrators was performed by Tom Steigauf and Mark Jones of Alliant Techsystems. Barmac Taleghani of the AMTL Materials Testing and Evaluation branch performed tensile and impact testing on Ultramet materials. Ultramet is grateful to all these individuals and organizations for their assistance with characterization of these new composite materials.

REFERENCES

1. R. Dowding (AMTL), communication with J. Stiglich (Ultramet), January 1992.

2. L. Magness and T. Ferrand, "Deformation Behavior and its Relationship to the Penetration Performance of High Density KE Penetrator Materials", presented at the Army Science Conference, Research Triangle Park, NC, June 1990.

3. R. Dowding, K. Tauer, P. Woolsey, and F. Hodi, "Metallurgical and Ballistic Characterization of Quarter-Scale Tungsten Alloy Penetrators", MTL TR-90-31 (Army Materials Technology Laboratory, Watertown, MA, May 1990).

4. J. Spencer and J. Mullendore, "Relationship Between Composition, Structure, Properties, Thermomechanical Processing, and Ballistic Performance of Tungsten Heavy Alloys", MTL TR-91-44 (Army Materials Technology Laboratory, Watertown, MA, November 1991).

5. R. German, "Microstructure and Impurity Effects on Tungsten Heavy Alloys", Final Report to Army Research Office for Period May 1987 to April 1990, July 1990.

6. R. Dowding, "Tungsten Heavy Alloys: A Tutorial Review", presented at Conference on P/M in Aerospace and Defense Technologies, Tampa, FL, March 1991; published in P/M in Aerospace and Defense Technologies (MPIF, 1991).

7. R. Dowding, "Tungsten Alloy Research at the U.S. Army Materials Technology Laboratory", presented at 1991 TMS Annual Meeting, New Orleans, LA, February 1991; published in Tungsten and Tungsten Alloys: Recent Advances, A. Crowson and E. Chen, eds. (The Metallurgical Society, 1991).

8. R. Dowding, "Recrystallization and Respheroidization of Tungsten Grains in a Tungsten Heavy Alloy", MTL TR-89-31 (Army Materials Technology Laboratory, Watertown, MA, April 1989).

9. R. Dowding and K. Tauer, "Strain Aging in Tungsten Heavy Alloys", MTL TR-89-63 (Army Materials Technology Laboratory, Watertown, MA, July 1989).

10. G. Allen, "Metal Injection Molding of Tungsten Heavy Alloys", MTL TR-91-37 (Army Materials Technology Laboratory, Watertown, MA, October 1991).

11. W. Bruchey and D. Montial, "Mechanical Property Evaluation of a Series of Commercial Tungsten Alloys", BRL-MR-3606 (Army Ballistics Research Laboratory, June 1987).

12. W. Bruchey, E. Horwath, and P. Kingman, "Orientation Dependence of Deformation and Penetration Behavior of Tungsten Single Crystal Rods", presented at 1991 TMS Annual Meeting, New Orleans, LA, February 1991; published in Tungsten and Tungsten Alloys: Recent Advances, A. Crowson and E. Chen, eds. (The Metallurgical Society, 1991).

13. U. Gerlach, "Microstructural Analysis of Residual Projectiles: A New Method to Explain Penetration Mechanisms", Met. Trans. A 17A (1986), 435.

14. Y. Kim, J. Park, and D. Yoon, "Liquid Flow into the Interior of W-Ni-Fe Compacts during Liquid Phase Sintering", Intl. J. Powder Met. and Powder Tech. 21 (1985), 29.

15. S. Jung, I. Moon, Y. Kwon, and J. Choi, "Press Forging of an Activated Sintered W-Powder Compact", Refractory and Heavy Metals (1987), 46.

16. L. Ekbom, "Deformation Behavior of High Density Tungsten Alloys", presented at the International Ballistics Conference, Shrivenham, U.K., April 1986.

17. R. Tham and A. Stilp, "Yield Strength and Flow Stress Measurements of Tungsten Sinter Alloys at Very High Strain Rates", J. de Phys. C3 49 (1988), 85.

18. R. Tham and A. Stilp, "Propagation of Compression Waves in Impacted Tungsten Sinter Alloys and Evaluation of the Dynamic Compression Strengths of these Materials", presented at 3rd Conference on Mechanical Properties at High Rates of Strain, Oxford, U.K., 1984.

19. D. Chaiat, "Future P/M Materials for Kinetic Energy Penetrators and Shaped Charge Liners", presented at Seminar on P/M in Defense Technology, Israel, December 1986.

20. J.G. Sheek, J.J. Stiglich, and J.T. Harding, "Coated Tungsten Powder", Final Report (ULT/TR-87-4831), Contract DAAL02-86-C-0112, Army Materials Technology Laboratory, Watertown, MA, March 1987.

21. W. Gurwell, "A Review of Embrittlement Mechanisms in Tungsten Heavy Alloys", presented at local TMS Meeting, Boston, MA, 1986.

22. R. German, L. Bourguignon, and B. Rabin, "Microstructure Limitations of High Tungsten Content Heavy Alloys", J. Metals (1985), 36.

23. H. Yoon et al., "Effect of Vacuum Treatment on Mechanical Properties of W-Ni-Fe Heavy Alloys", J. Mater. Res. Sci. 18 (1983), 1374.

24. W. Northcutt, "Fabrication Development of Tungsten Alloy Penetrators", ORNL-TR-Y-1994 (Oak Ridge National Laboratories, Oak Ridge, TN, 1975).

25. C. Powell, J. Oxley, and J. Blocher Jr., eds., Vapor Deposition (John Wiley & Sons, New York, 1966).

26. D. Kunii and O. Levenspiel, Fluidization Engineering (John Wiley & Sons, New York, 1966).

27. S. Mulligan and R. Dowding, "Sinterability of Tungsten Powder CVD Coated with Nickel and Iron", MTL TR-90-56 (Army Materials Technology Laboratory, Watertown, MA, November 1990).

28. B.E. Williams, J.J. Stiglich, and R.B. Kaplan, "Improved Composite Powder Fabrication", presented at 15th Annual Conference on Composites and Advanced Ceramics, Cocoa Beach, FL, 13-16 January 1991.

29. B.E. Williams, J.J. Stiglich, and R.B. Kaplan, "CVD Coated Tungsten Powder Composites I: Processing and Characterization", presented at 1991 TMS Annual Meeting, New Orleans, LA, February 1991; published in Tungsten and Tungsten Alloys: Recent Advances, A. Crowson and E. Chen, eds. (The Metallurgical Society, 1991).

30. J.J. Stiglich, B.E. Williams, and R.B. Kaplan, "CVD Coated Tungsten Powder Composites II: Fabrication and Properties", presented at 1991 TMS Annual Meeting, New Orleans, LA, February 1991; published in Tungsten and Tungsten Alloys: Recent Advances, A. Crowson and E. Chen, eds. (The Metallurgical Society, 1991).

31. B.E. Williams and J.J. Stiglich, "Hafnium- and Titanium-Coated Tungsten Powders for Kinetic Energy Penetrators", Final Report (ULT/TR-91-7670), Contract DAAL04-91-C-0022, Army Materials Technology Laboratory, Watertown, MA, October 1991.

32. B.E. Williams, J.J. Stiglich, R.B. Kaplan, and R.H. Tuffias, "A Major Advance in Powder Metallurgy", presented at 2nd National Technology Transfer Conference (Technology 2001), San Jose, CA, December 1991; published in Conference Proceedings, NASA CP-3136, Vol. 1.

33. B.E. Williams, J.J. Stiglich, R.B. Kaplan, and R.H. Tuffias, "The Coating of Powders by Chemical Vapor Deposition", presented at 1991 MRS Fall Meeting, Boston, MA, 2-6 December 1991.

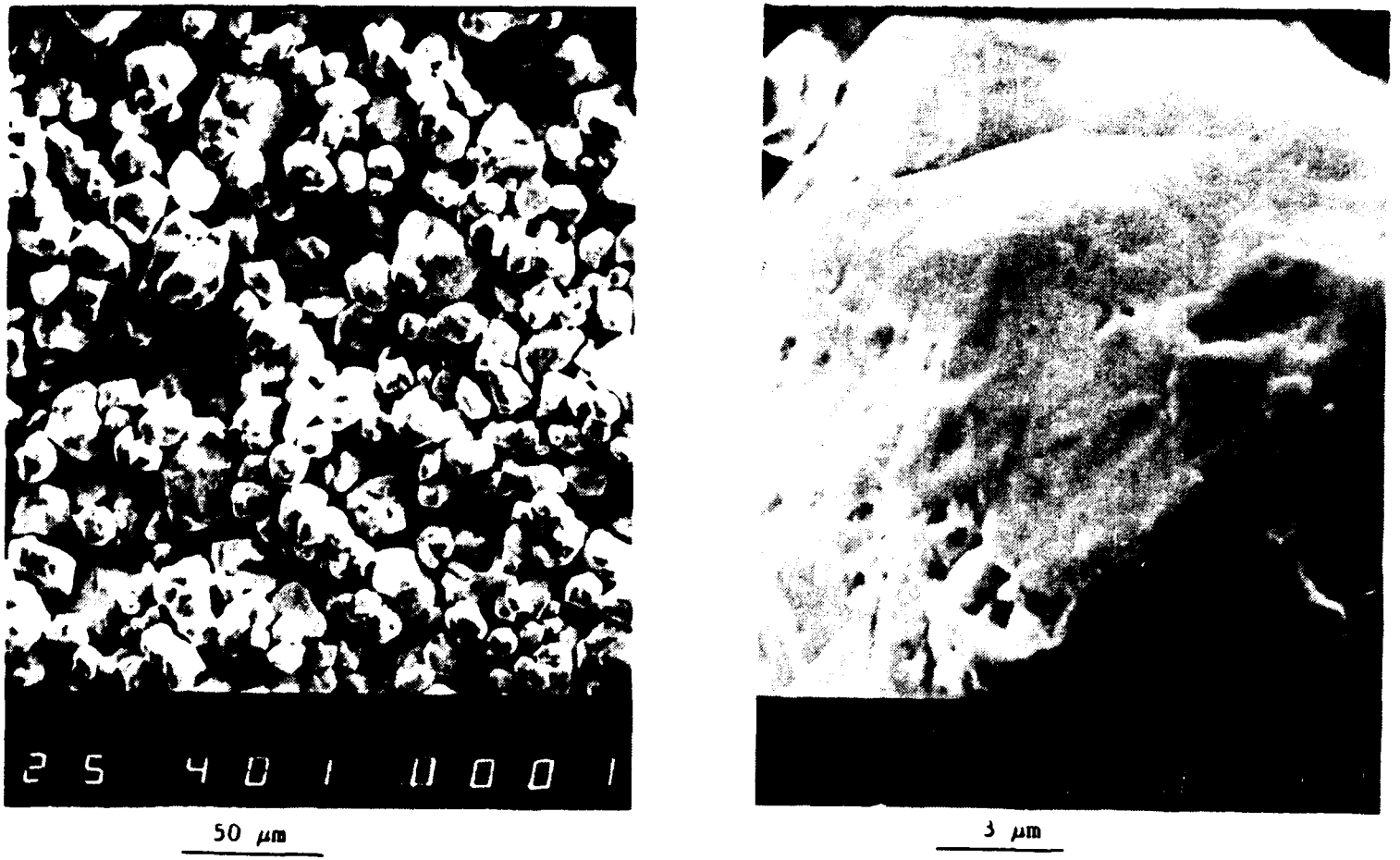

Figure 1. SEM micrographs of uncoated (as-received) 12-μm tungsten powder, showing uniformity of particle size, lack of sharp edges and agglomeration, and smooth surface morphology (left, 400x; right, 6000x)

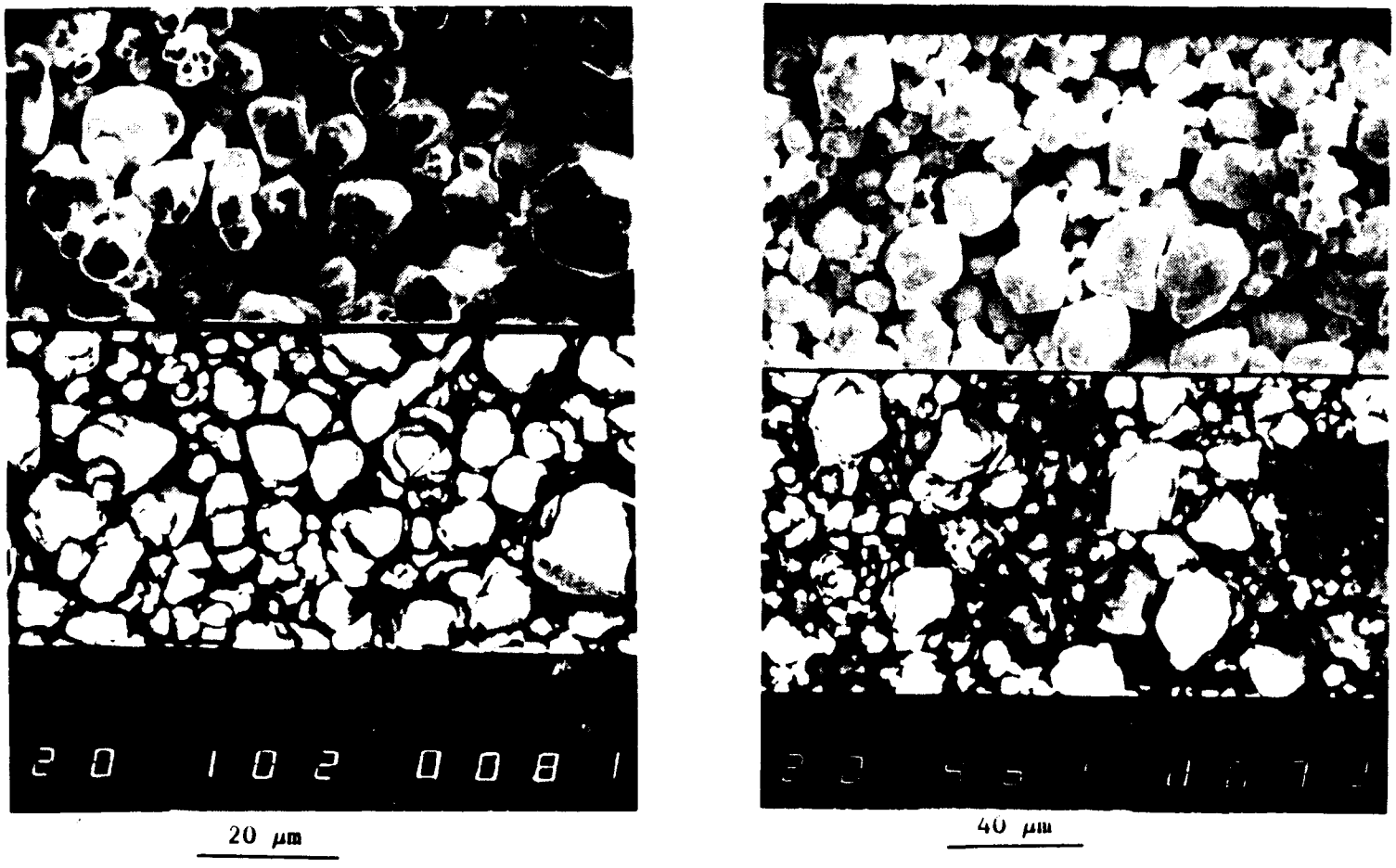

Figure 2. SEM micrographs of coated (W:4.3%Ni:1.7%Fe) powder, with secondary electron image (SEI) at top and backscattered electron image (BEI) at bottom. SEI indicates surface morphology, while BEI emphasizes compositional (elemental) differences.
A. Little contrast evident in BEI, indicating uniform coating (1000x)
B. Extreme contrast evident in BEI, indicating nonuniform coating (480x)

Figure 3. SEM micrograph of surface of individual grain of coated (W:4.3%Ni:1.7%Fe) powder at high magnification (20,000x)

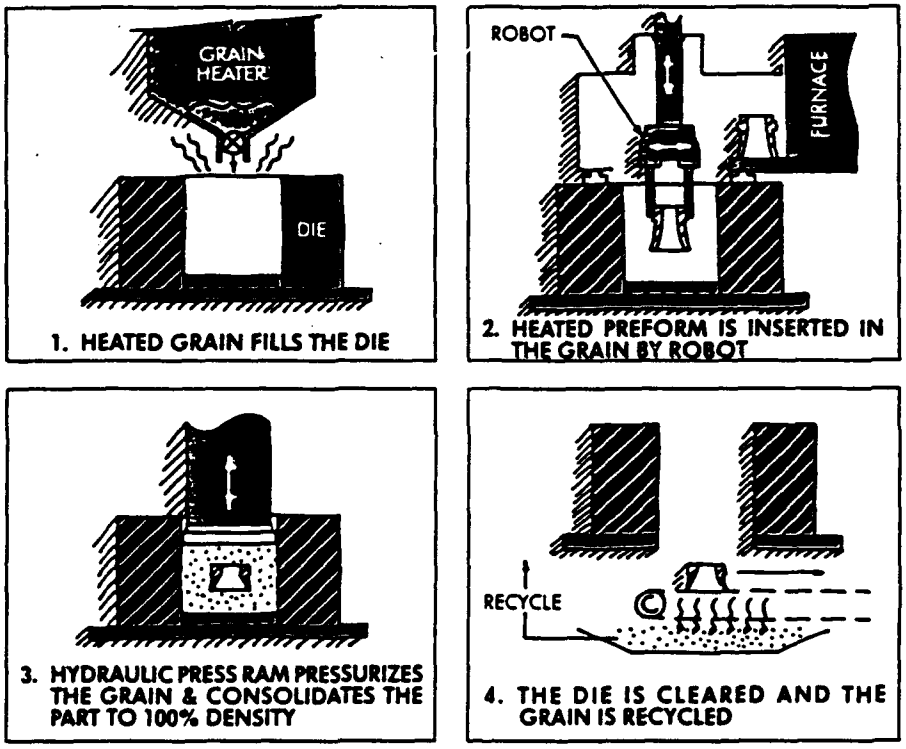

Figure 4. Schematic of Ceracon® consolidation process

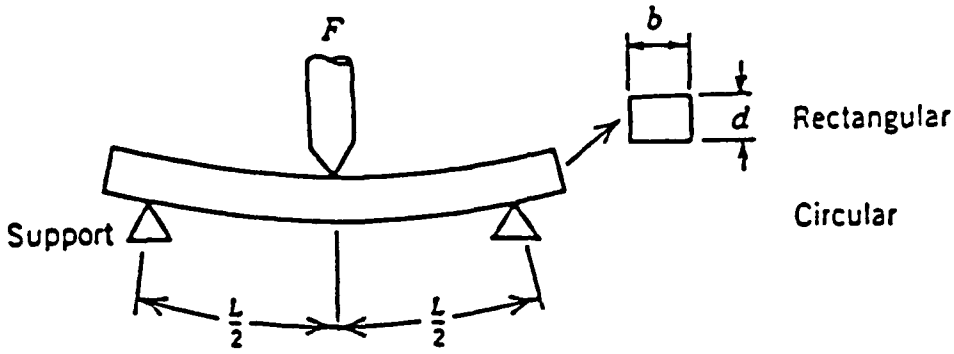

σ = Stress = $\frac{Mc}{I}$

where M = Maximum bending moment

c = Distance from center of specimen to outer fibers

I = Moment of inertia of cross section

F = Applied load

	$\frac{M}{}$	$\frac{c}{}$	$\frac{I}{}$	$\frac{\sigma}{}$	$\frac{E}{}$
Rectangular	$\frac{FL}{4}$	$\frac{d}{2}$	$\frac{bd^3}{12}$	$\frac{3FL}{2bd^2}$	$\frac{FL^3}{4\delta bd^3}$

E = elastic modulus

δ = deflection

Figure 5. Three-point loading scheme used to measure flexural strength and midspan deflection of consolidated tungsten powder composites

NOTES:

1. DIMENSIONS IN INCHES, UNLESS NOTED.

2. TOLERANCES, UNLESS NOTED.

SQUARENESS	⊥ PERPENDICULAR	± .001 TIR
	∥ PARALLEL	± .001 TIR
DIAMETERS	◎ CONCENTRIC TO -A-	± .001 TIR
FRACTIONS		± 1/64
DECIMAL	.XX	± .005
	.XXX	± .001
	.XXXX	± .0005

TYPE	A	B	C	D_1	D_2	G	F	J	R
TR 1	4-3/4	3.0	2-1/4	.505	.510	2.00	7/8	3/4-16-2A	3/8
TR 2A	3-5/8	2-1/4	1-3/4	.357	.360	1.40	11/16	1/2-16/2A	1/4
TR 2B	3-5/8	2-1/4	1-3/4	.357	.360	1.40	11/16	3/4-16-2A	1/4
TR 3A	2-7/8	1-5/8	1-1/4	.252	.254	1.00	5/8	3/8-16-2A	3/16
TR 3B	2-7/8	1-5/8	1-1/4	.252	.254	1.00	5/8	1/2-16-2A	3/16
TR 4	2-7/8	1-5/8	1-1/4	.212	.214	.90	5/8	3/8-16-2A	3/16
TR 5	2-1/4	1-1/4	1-3/4	.160	.162	.64	1/2	5/16-24-2A	1/8
TR 6	1-5/8	13/16	5/8	.113	.114	.45	13/32	1/4-20-2A	3/32

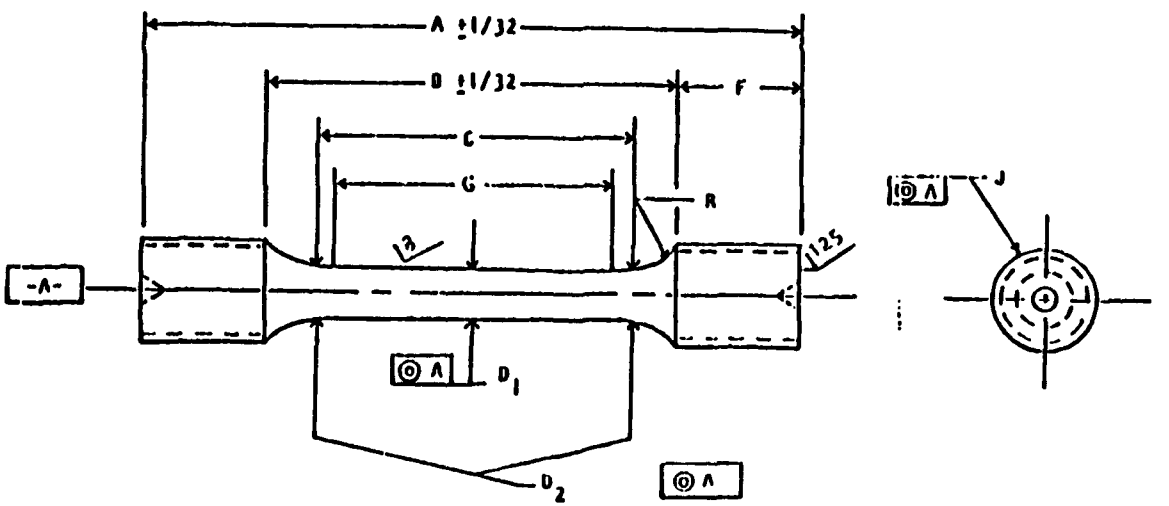

Figure 6. Schematic of tensile test specimen

NOTES:

1. DIMENSIONS IN INCHES, UNLESS NOTED.

2. TOLERANCES, UNLESS NOTED.

SQUARENESS	⊥ PERPENDICULAR	± .001 TIR
	∥ PARALLEL	± .001 TIR
DIAMETER;	Ⓜ CONCENTRIC TO -A-	± .001 TIR
FRACTIONS		± 1/64
DECIMAL	.XX	± .005
	.XXX	± .001
	.XXXX	± .0005

TYPE	A	G	N	R	T	n
CV 1	6.500	1.182	.946	.010	1.182	45°
CV 2	2.165	.394	.315	.010	.394	45°
CV 3	2.165	.394	.315	.010	.295	45°
CV 4	2.165	.394	.315	.010	.197	45°
CV 5	2.165	.394	.315	.010	.098	45°
CV 6	2.165	.295	.237	.010	.295	45°
CV 7	2.165	.197	.158	.010	.788	45°
CV 8	2.165	.197	.158	.010	.394	45°
CV 9	2.165	.197	.158	.010	.197	45°
CV 10	2.165	.118	.094	.010	.394	45°
CV 11	1.080	.197	.158	.010	.394	45°
CV 12	1.080	.197	.158	.010	.197	45°

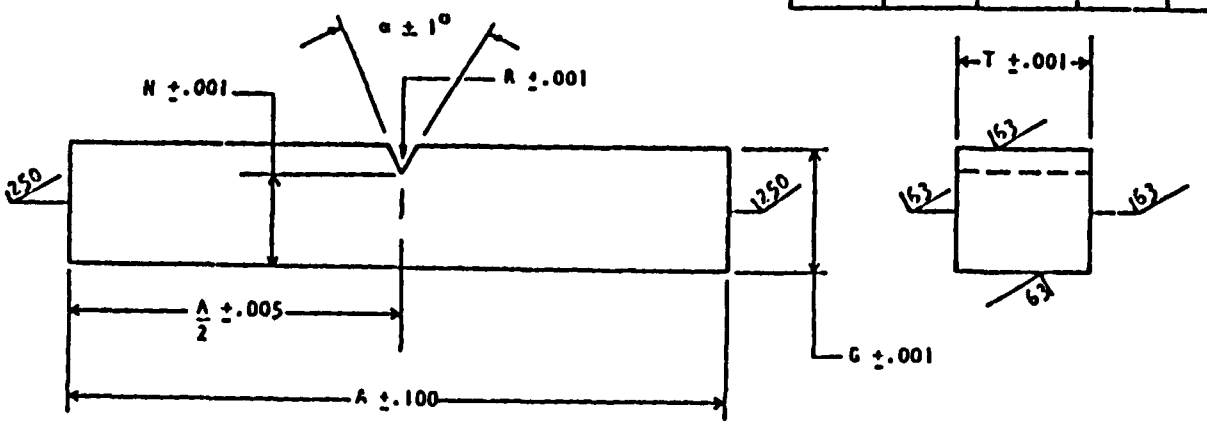

Figure 7. Schematic of Charpy impact test specimen

Figure 8. SEM micrograph of commercially available W:7.0%Ni:3.0%Fe composite, fabricated by conventional powder mixing and consolidated by LPS, showing extensive non-homogeneous matrix distribution and tungsten-tungsten particle contact (400x)

Figure 9. SEM micrograph of Ultramet-coated W:3.5%Ni:1.2%Fe composite consolidated by HIP, showing pooling of matrix between tungsten grains and extensive tungsten-tungsten particle contact (2000x)

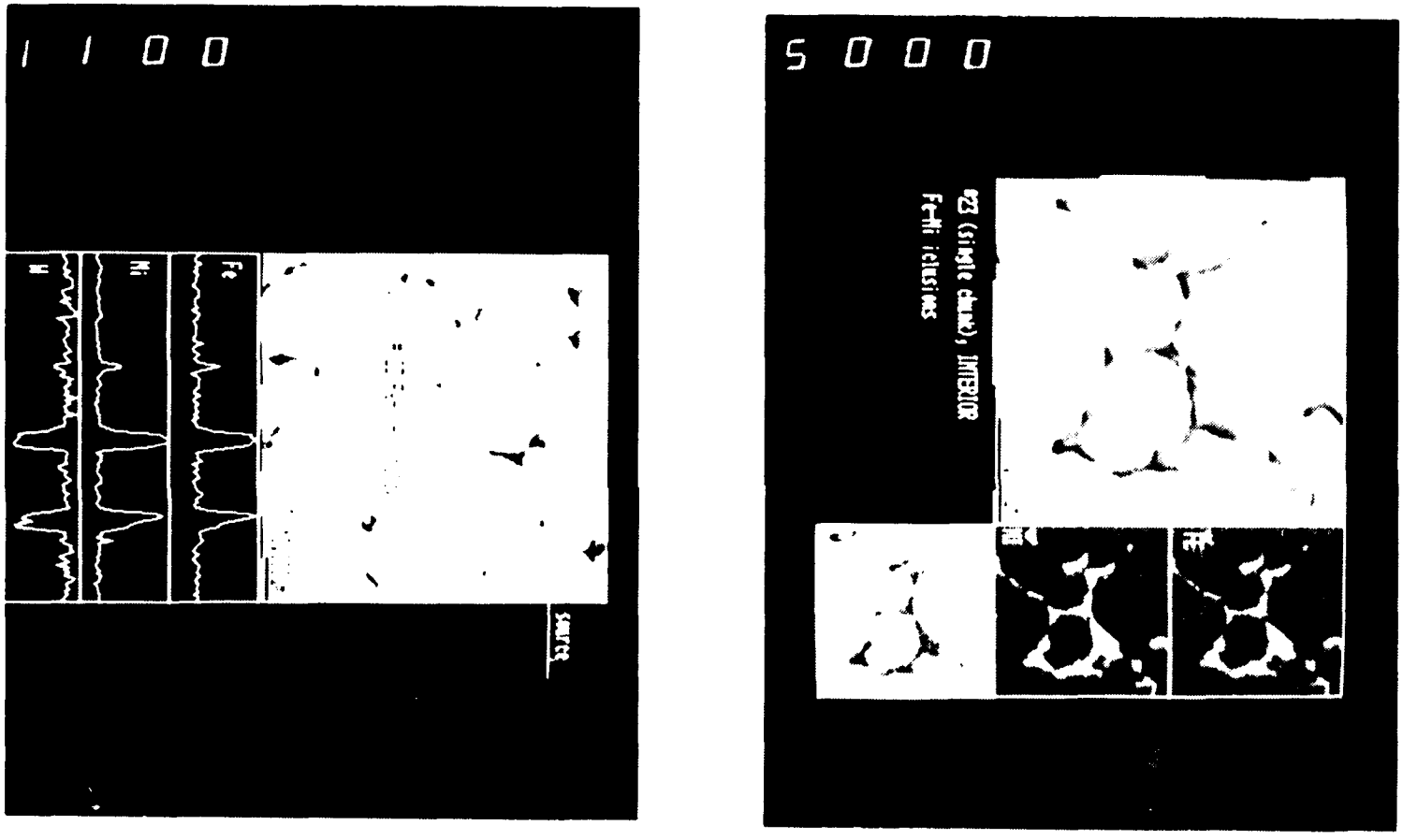

Figure 10. EDX line scan (left) and elemental map (right) of Ultramet-coated W:3.5%Ni:1.2%Fe composite consolidated by HIP, showing nonuniformity of matrix distribution

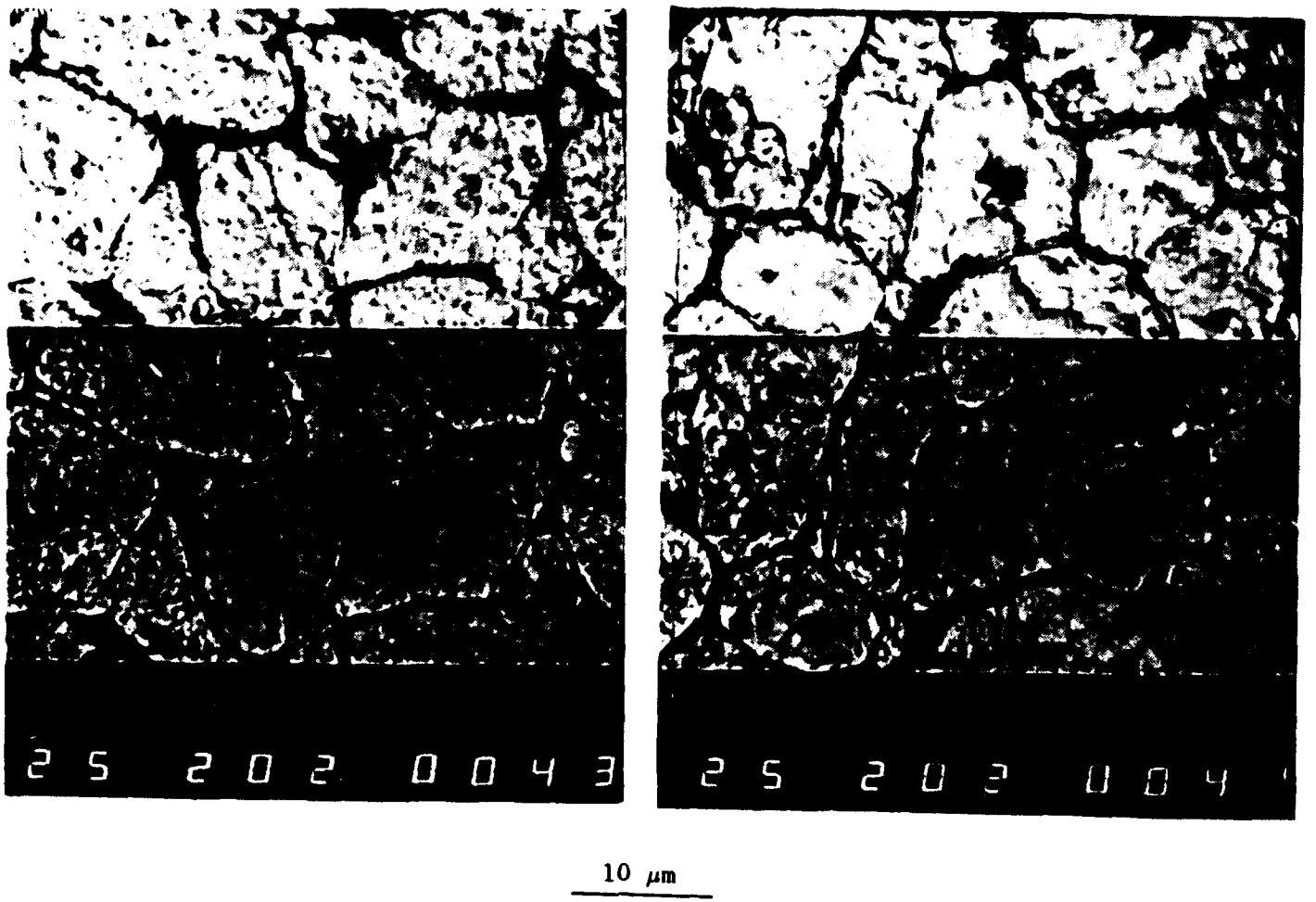

Figure 11. SEM micrographs of Ultramet-coated W:3.5%Ni:1.5%Fe composites consolidated by Ceracon (small billet), with SEI at top and BEI, showing uniformity of matrix distribution, at bottom (2000x)

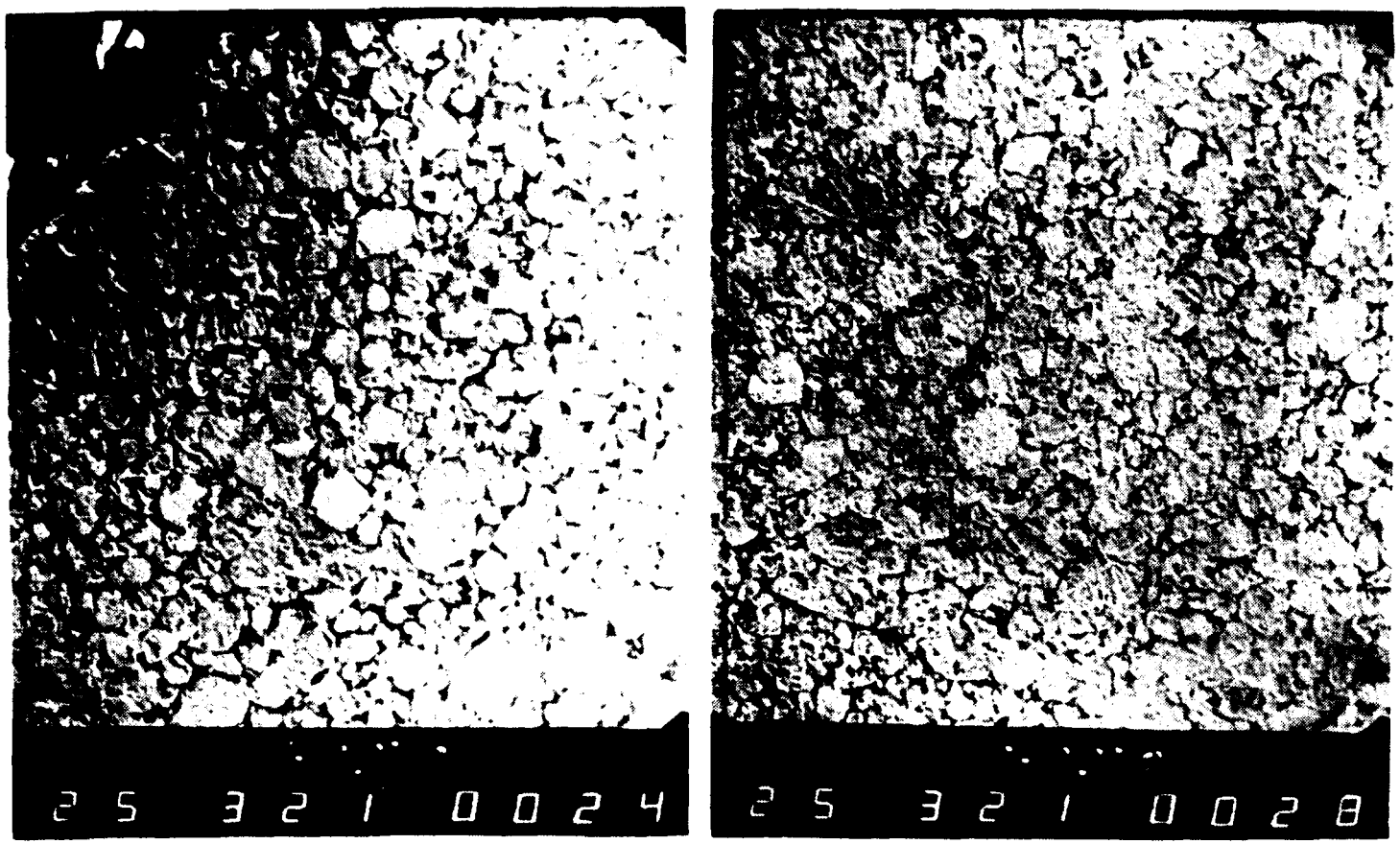

Figure 12. SEM micrographs of Ultramet-coated W:3.5%Ni:1.5%Fe composite consolidated by Ceracon (small billet), showing porous outer region of billet near surface (left) and virtually pore-free region at center of billet (right) (320x)

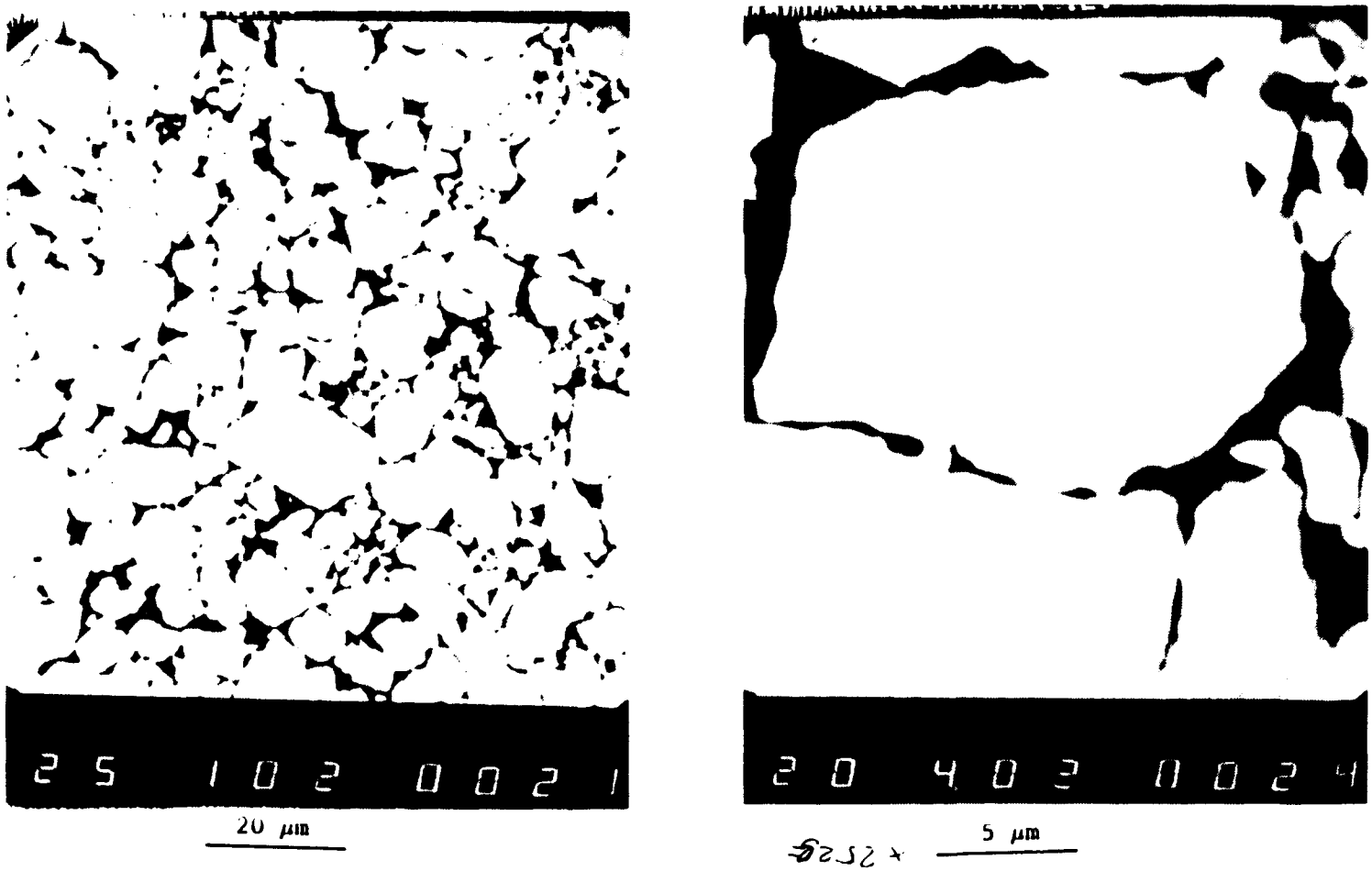

Figure 13. SEM micrographs of Ultramet-coated W:4.3%Ni:1.7%Fe composite consolidated by quasi-optimized Ceracon process (large billet)

A: Lower magnification, showing relatively good matrix distribution but with some tungsten-tungsten particle contact apparent (1000x)

B: Higher magnification, showing a degree of matrix between tungsten grains that appear to be in contact at lower magnification (4000x)

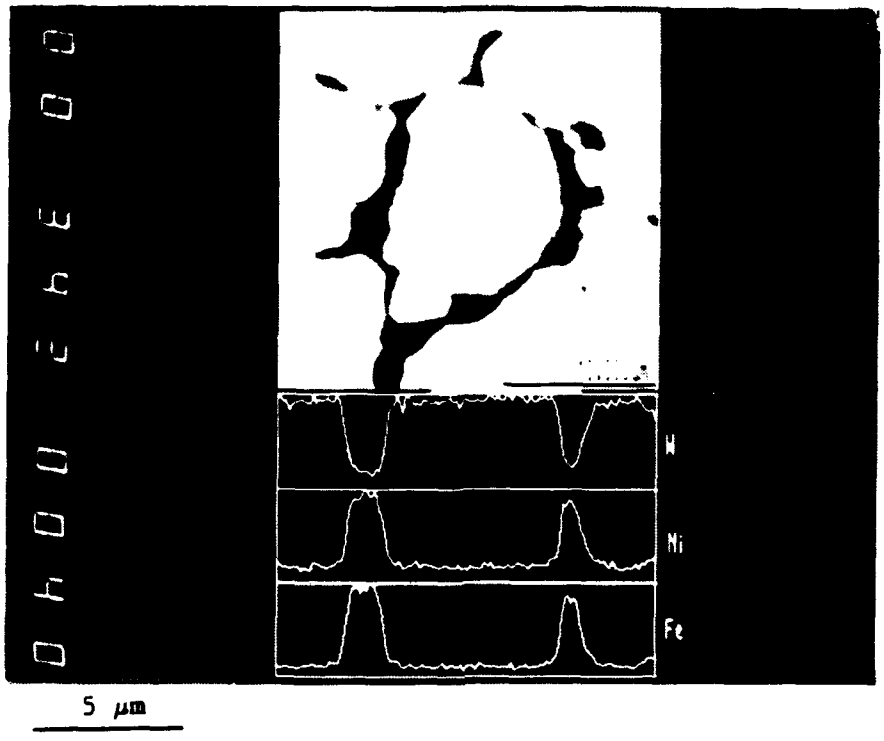

Figure 14. EDX line scan across Ultramet-coated W:4.3%Ni:1.7%Fe composite, consolidated by Ceracon, clearly showing variance in composition from Ni/Fe matrix coating to tungsten powder particle (3900x)

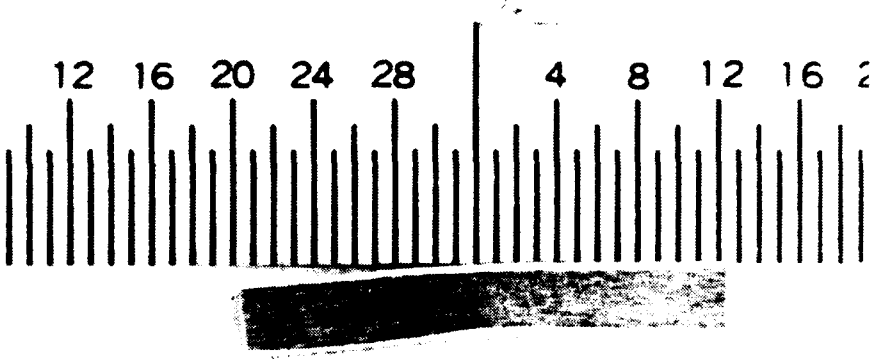

Figure 15. Photograph of W:4.3%Ni:1.7%Fe composite flexural specimen for which three-point loading test was aborted just prior to expected fracture in order to show degree of bending

Figure 16. SEM micrograph of Ultramet-coated W:3.5%Ni:1.5%Fe composite consolidated by HIP, showing poor matrix distribution and resultant intergranular fracture (2000x)

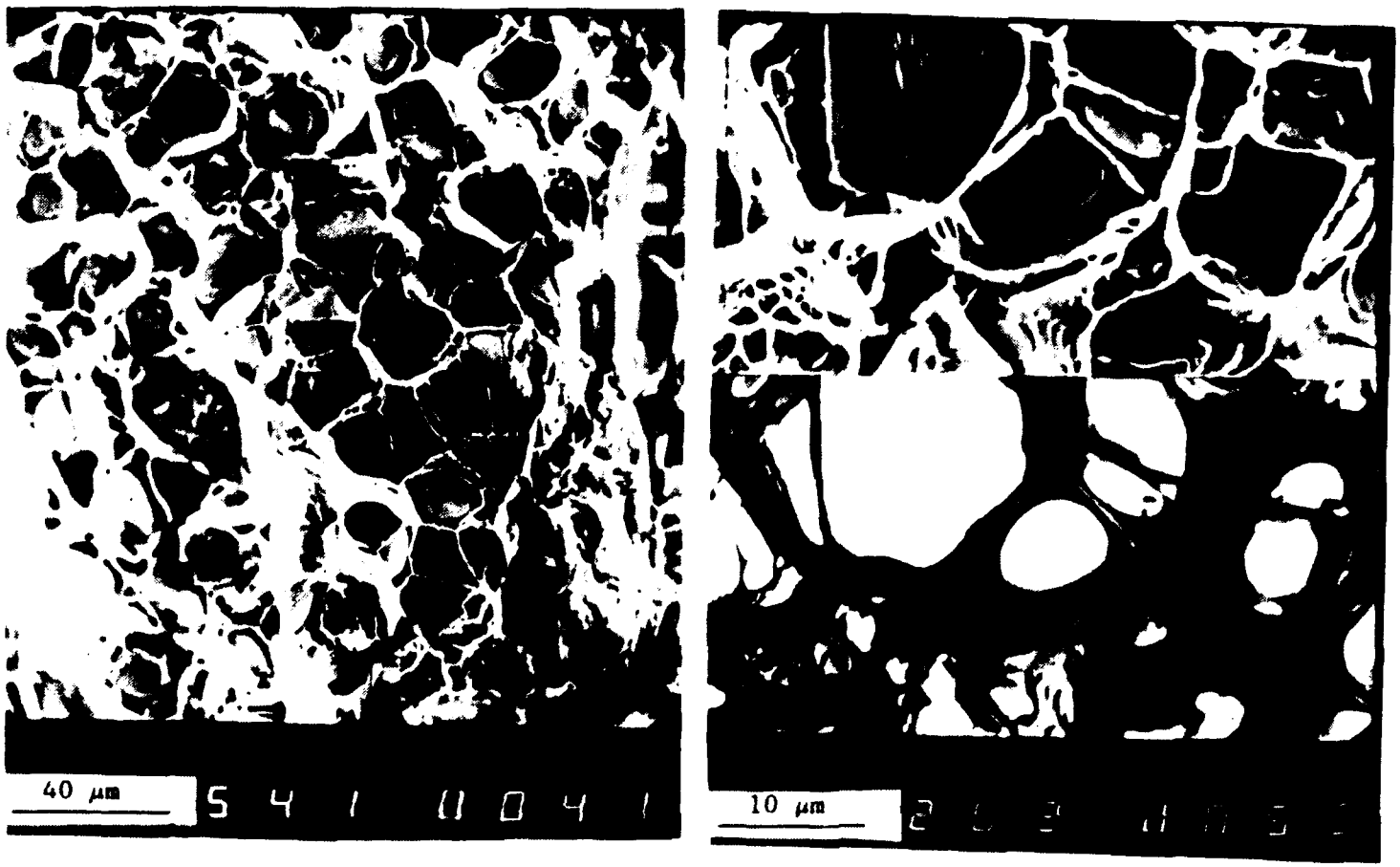

Figure 17. SEM micrographs of commercially available W:7.0%Ni:3.0%Fe composite consolidated by LPS
A: Poor matrix distribution and resultant intergranular fracture originating at flat surfaces seen on individual tungsten grains (540x)
B: Shiny flat surfaces on individual tungsten grains (BEI, bottom) were areas of tungsten-tungsten particle contact prior to fracture; no sign of matrix material is evident in these areas (2000x)

Figure 18. SEM micrograph of Ultramet-coated W:3.5%Ni:1.5%Fe composite consolidated by Ceracon, showing significant intragranular failure and grain pullout in addition to intergranular fracture (1000x)

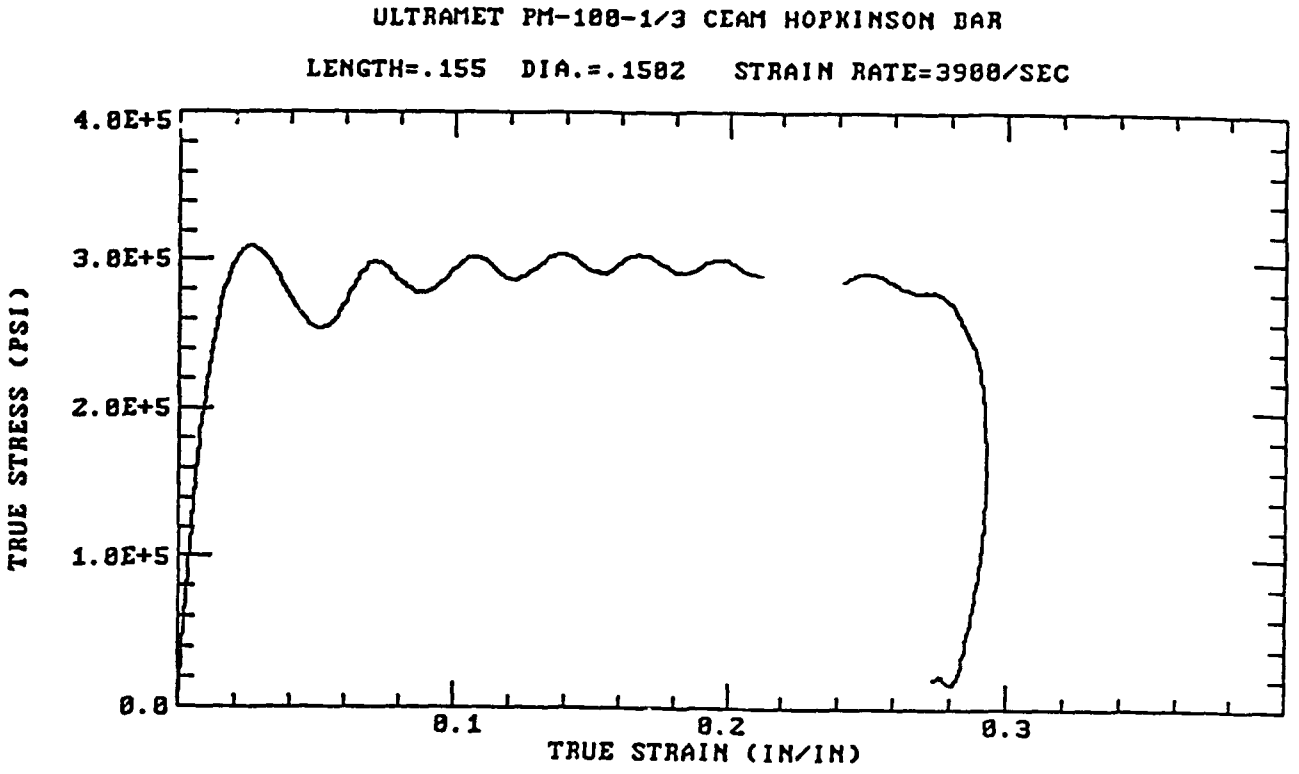

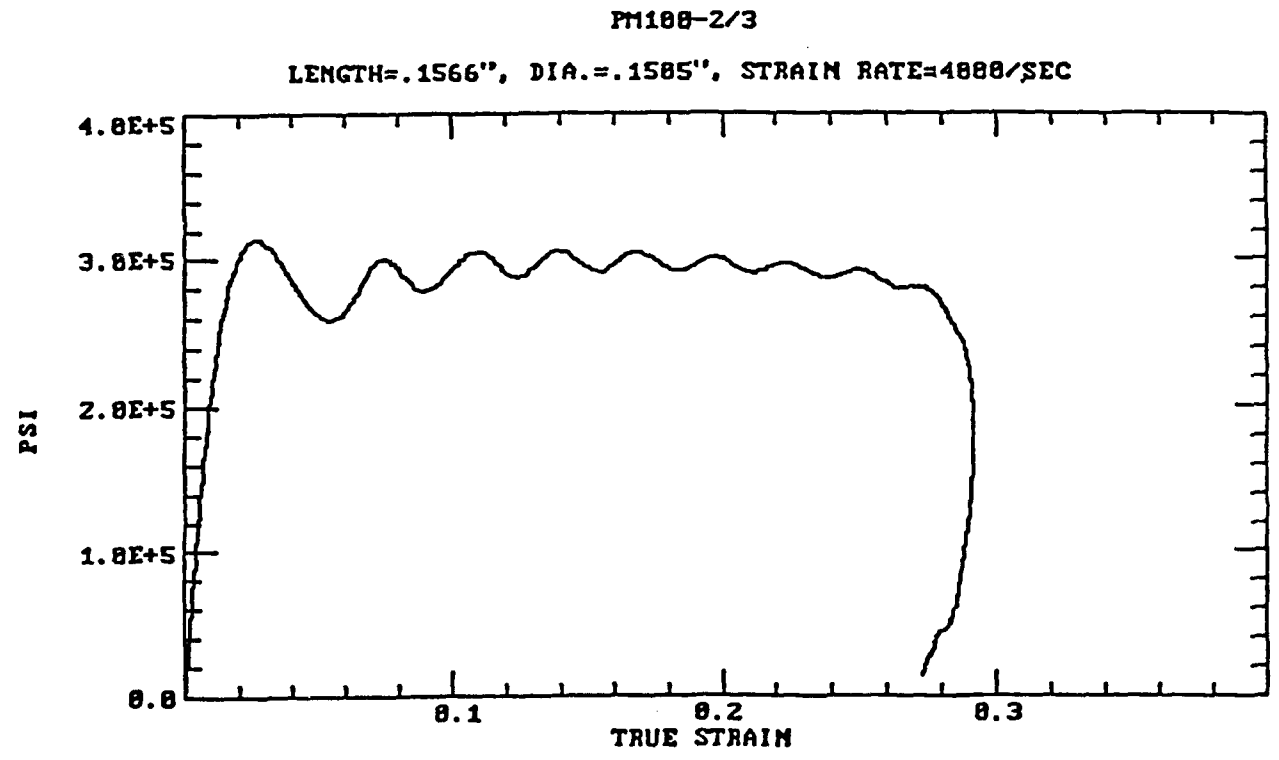

Figure 19. Elevated strain rate plots of true stress vs. true strain for Ultramet-coated W:3.8%Ni:1.3%Fe composites consolidated by HIP, measured at 3900/sec (top) and 4000/sec (bottom)

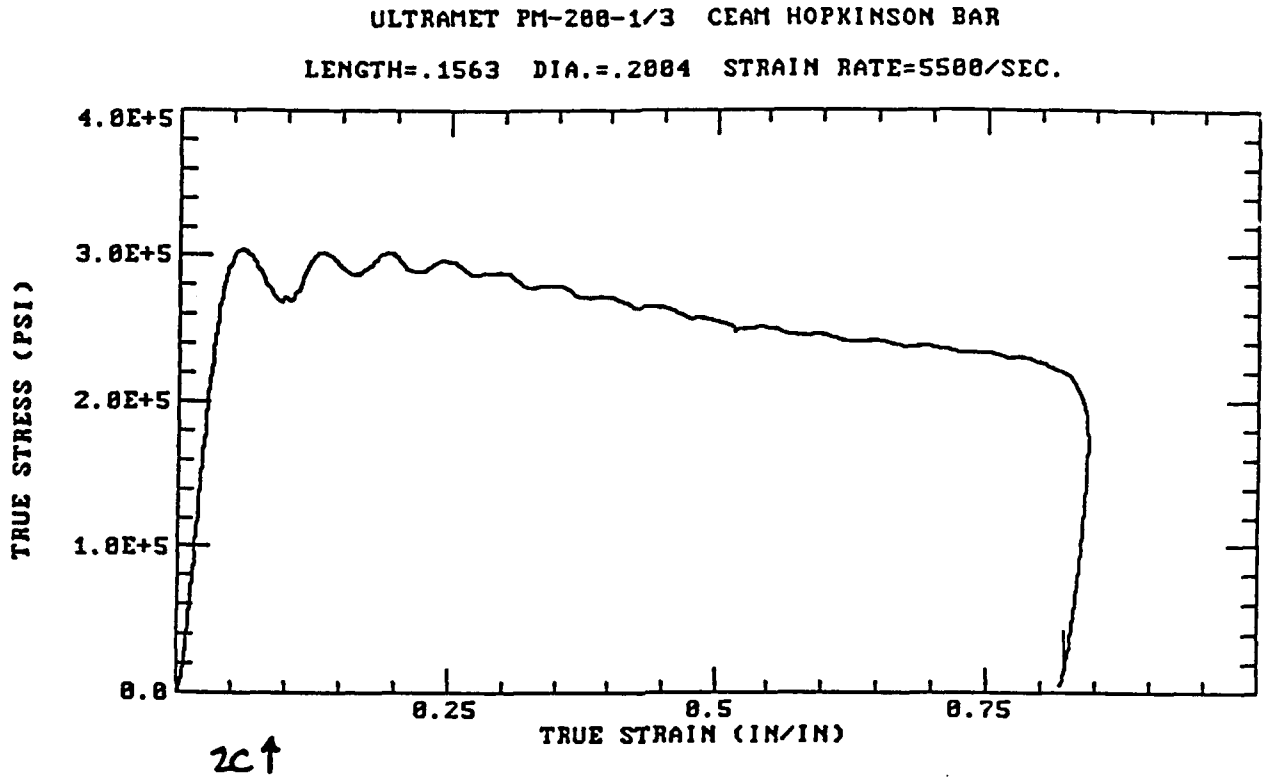

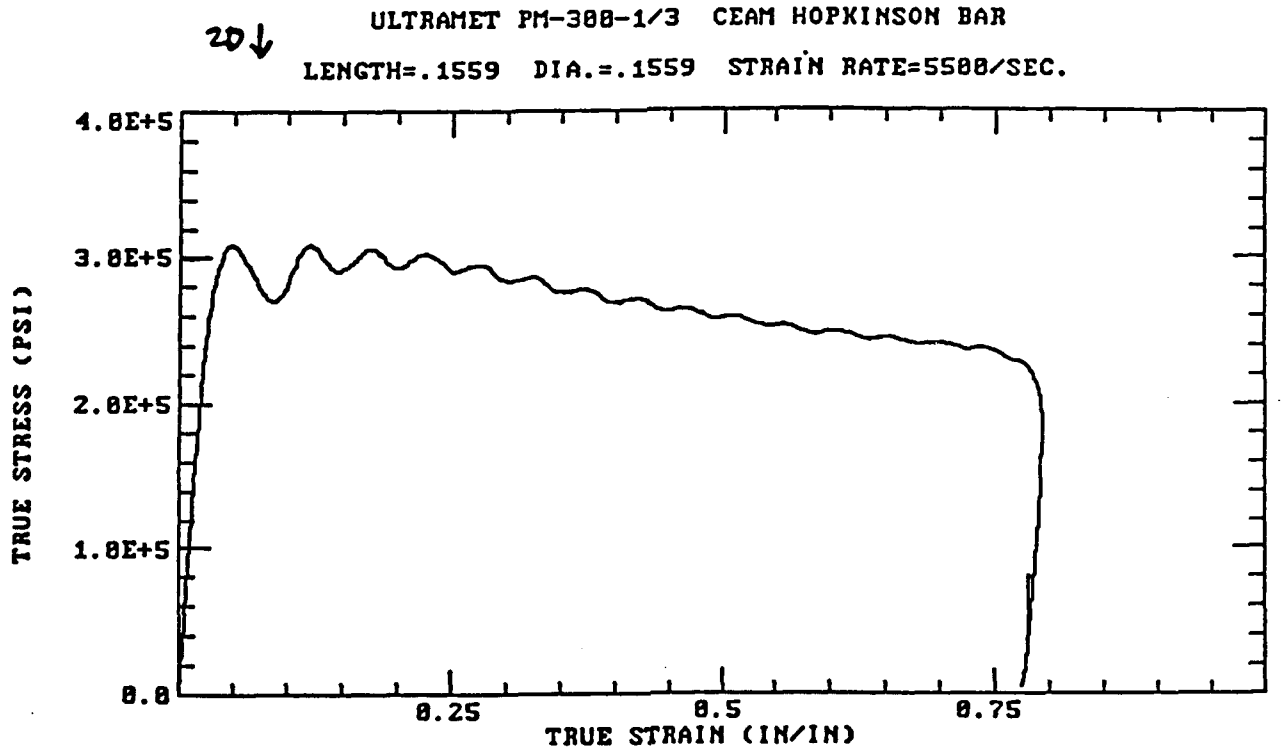

Figure 20. Elevated strain rate plots of true stress vs. true strain for Ultramet-coated W:3.5%Ni:1.2%Fe composites consolidated by HIP, measured at 5500/sec, with 5 wt% uncoated 5-μm tungsten powder added (top) and 10 wt% uncoated 5-μm tungsten powder added (bottom)

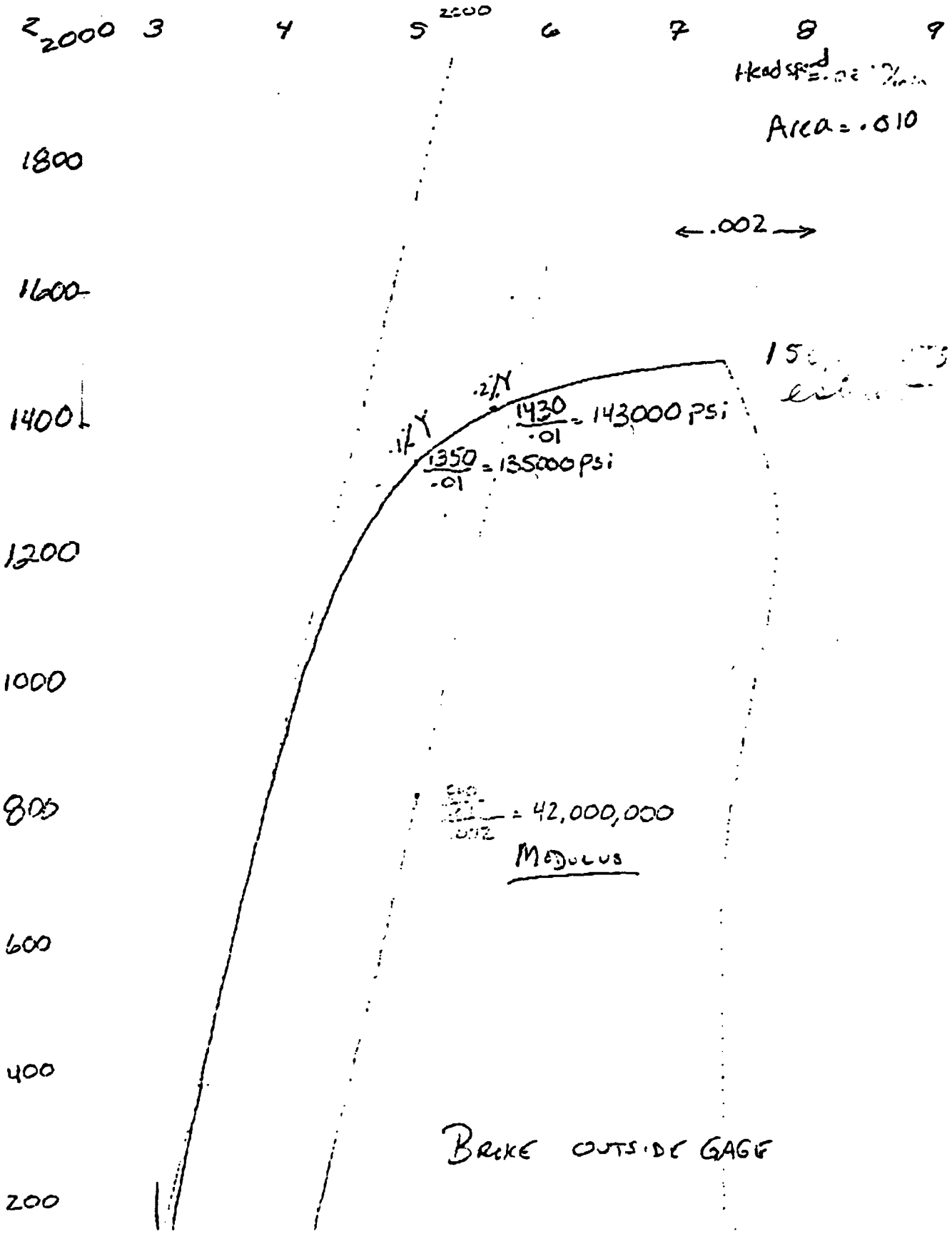

Figure 21. Typical load vs. elongation data obtained in tensile testing at AMTL, showing only limited ductility in Ultramet-coated W:4.3%Ni:1.7%Fe composites consolidated by Ceracon

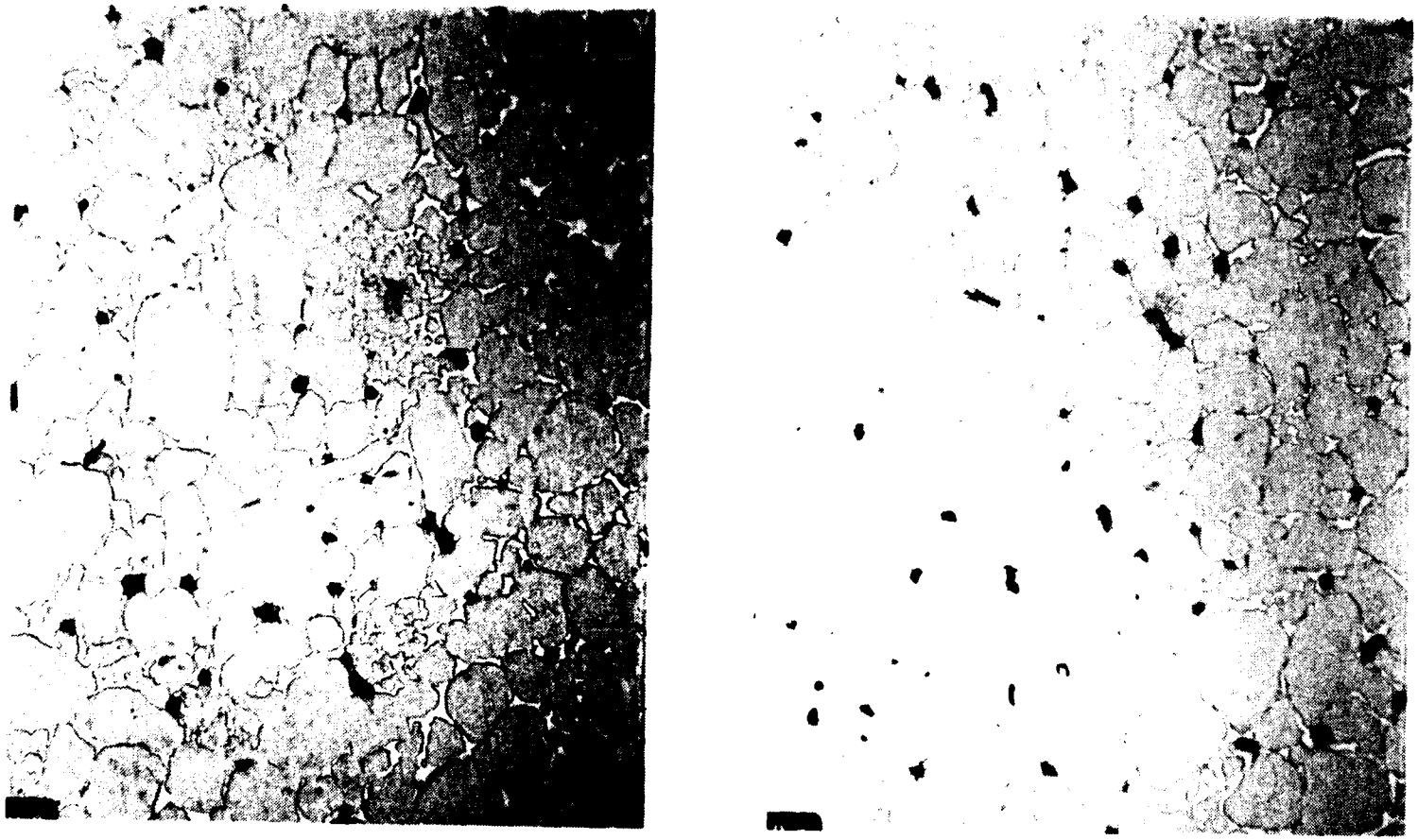

Figure 22. Optical micrographs of Ultramet-coated/Ceracon-consolidated W_p composite ballistic test specimens, showing 0.5-1.0 vol% surface porosity (500x)

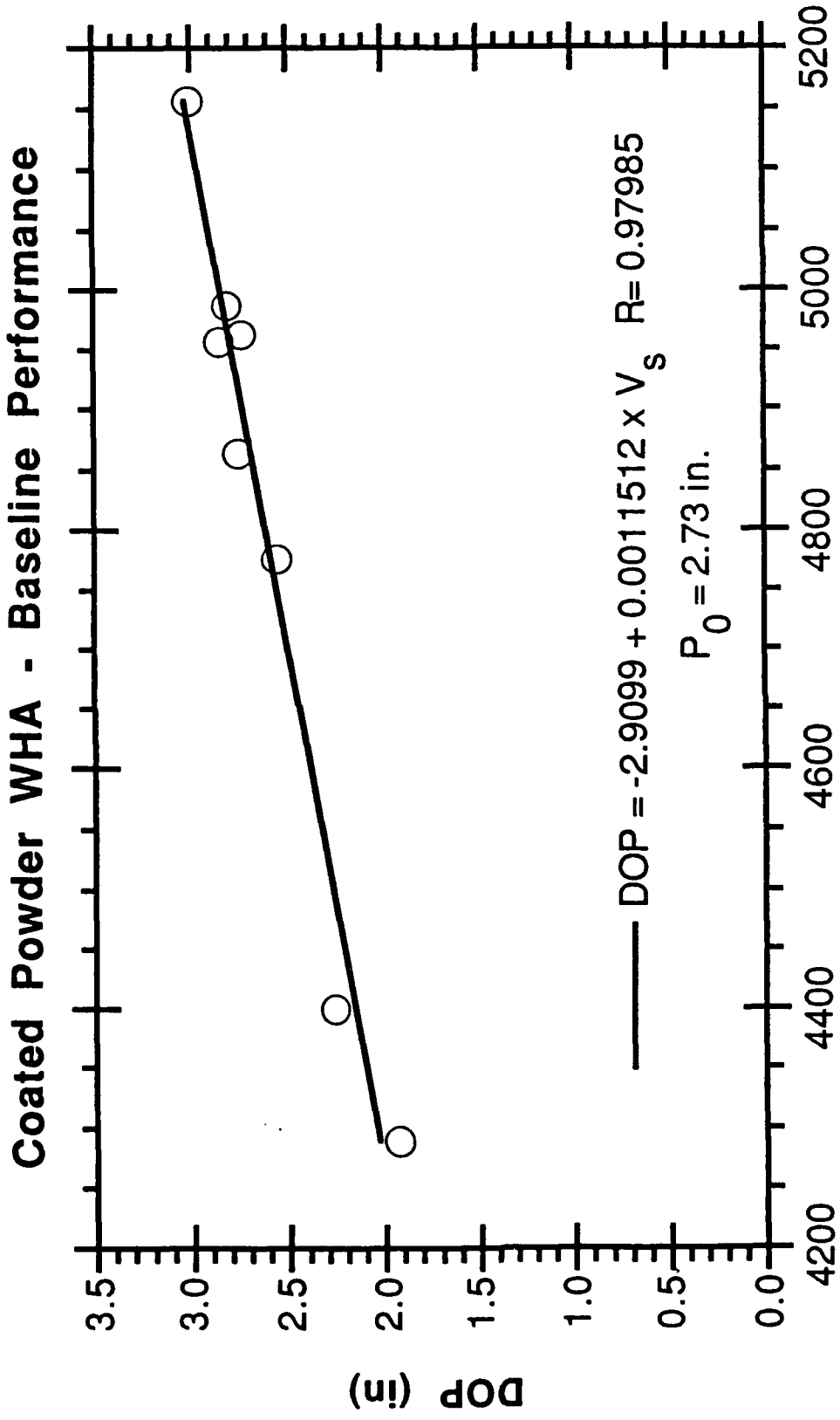

Figure 23. Depth of penetration vs. velocity data obtained in ballistic testing of Ultramet W_p composite material at AMTL

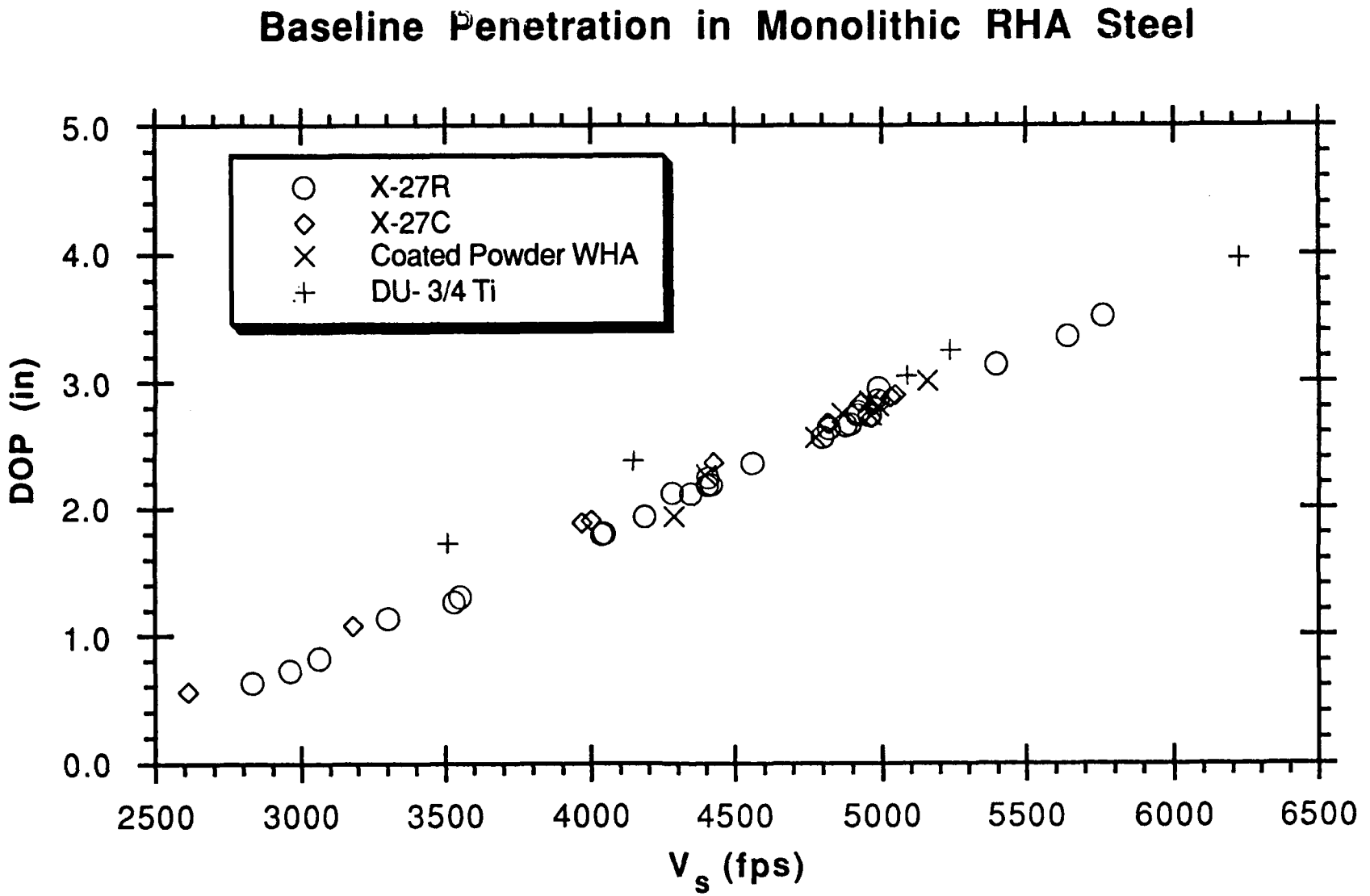

Figure 24. Depth of penetration vs. velocity data obtained in ballistic testing of Ultramet W_p composites, two other tungsten composites, and DU at AMTL

Table I. Powder Coating Programs at Ultramet

Description (coating on powder)	Application
3-4 wt% nickel/1-2 wt% iron on 12-μm tungsten	Ordnance
5-50 wt% copper on 100-μm AlN	High-conductivity composites
10-30 wt% aluminum on 5-μm TiB_2	Dispersion strengthening
TiB_2 on 5-μm aluminum	Dispersion strengthening
80 wt% tungsten on 150-μm Al_2O_3	Proprietary
10 wt% Al_2O_3 on 100-μm SiC	Ceramic composites
20 wt% titanium on 100-μm Al_2O_3	Proprietary
5 wt% iron on 100-μm WC	Cutting tools
3 wt% cobalt on 10-μm WC	Cutting tools
3 wt% iron on 20-500-μm diamond	Cutting tools
10-20 wt% hafnium and titanium on 12-μm tungsten	Ordnance

Table II. Specifications for M-68 De-Agglomerated Tungsten Powder

SUBJECT: BALL MILLED M-68 POWDER

LOT No.	ORIGINAL FEED (WA68-379C)	BALL MILLED 6 HRS (D-7035)
FSSS :	17.9 microns	14.3 microns
BULK DENSITY :	95.5 gm/in3	149.9 gm/in3
OXYGEN :	180 ppm	240 ppm
IRON :	3 ppm	32 ppm
NICKEL :	3 ppm	22 ppm
CHROMIUM :	7 ppm	17 ppm

MICROTRAC:

RANGE (micron)	(UNMILLED) PERCENT	(MILLED) PERCENT
176-125	0.0	0.0
125-88	4.4	0.0
88-62	9.4	0.0
62-44	19.5	2.7
44-31	25.9	12.5
31-22	20.9	16.5
22-16	10.6	22.4
16-11	7.0	24.5
11-7.8	1.5	11.0
7.8-5.5	0.8	5.7
5.5-3.9	0.0	3.0
3.9-2.8	0.0	1.5
2.8-1.9	0.0	0.2
1.9-1.4	0.0	0.0

Table III. Impurity Analysis of Powder Samples

Material	C (ppm)	O (ppm)
Pure 5-μm tungsten powder, as-received	30	780
Pure 5-μm tungsten powder, following heat treatment in hydrogen for one hour	<10	240
Pure 20-μm tungsten powder, as-received	50	540
Pure 20-μm tungsten powder, following heat treatment in hydrogen for one hour	<20	170
Coated 5-μm tungsten powder (W:3.5Ni:1.5Fe)	<10	380
Coated 20-μm tungsten powder (W:3.5Ni:1.5Fe)	<10	320

Note: Five (5) samples of each material tested; average values presented; variation in C values <10% within each group of five samples; variation in O values <15% within each group of five samples.

Table IV. Procedures, Reporting Limits, and Precision for Chemical Analysis

Element	Procedure	Estimated relative precision (%)	Normal low reporting limits (ppm)
Carbon	Combustion/IR: combustion of sample in oxygen, measuring evolved CO_2 by infrared	5	30
Oxygen	IGF/GC: inert gas fusion with gas chromatograph separation of gases using thermal conductivity or infrared readout	5	50
Tungsten	OES: optical emission spectroscopy	5	25
Hafnium	OES	5	25
Titanium	DCPS: direct current plasma source spectroscopy	5	35

Table V. Flexure Test Results for Ultramet-Coated/HIP-Consolidated Material

Length (in) (mm)	0.5625 14.288	0.5625 14.288	0.5625 14.288	0.5625 14.288	0.5625 14.288	0.5625 14.288	0.5625 14.288	0.5625 14.288	0.5625 14.288	0.5625 14.288
Width (in) (mm)	0.1903 4.834	0.1911 4.854	0.1907 4.844	0.1908 4.846	0.1921 4.879	0.1992 5.060	0.1913 4.859	0.1924 4.887	0.1903 4.834	0.1894 4.811
Depth (in) (mm)	0.1586 4.028	0.1600 4.064	0.1589 4.036	0.1594 4.049	0.1586 4.028	0.1586 4.028	0.1629 4.138	0.1558 3.957	0.1630 4.140	0.1590 4.039
Composition: %W %Ni %Fe % uncoated 5-μm tungsten powder	100.0 0.0 0.0 0.0	99.5 0.3 0.2 0.0	97.0 2.0 1.0 0.0	97.0 2.0 1.0 0.0	94.9 3.8 1.3 0.0	94.9 3.8 1.3 0.0	95.2 3.6 1.2 5.0	95.2 3.6 1.2 5.0	95.3 3.5 1.2 10.0	95.3 3.5 1.2 10.0
Consolidation	HIP	HIP	HIP	HIP	HIP	HIP	HIP	HIP	HIP	HIP
Measured Density (g/cm^3)	16.52	16.97	18.23	18.26	17.91	17.91	18.10	18.10	18.24	18.24
Theoretical Density (g/cm^3)	19.30	19.12	18.59	18.59	18.15	18.15	18.22	18.22	18.24	18.24
Percent Dense	85.6	88.8	98.0	98.2	98.7	98.7	99.7	99.7	100.0	100.0
Deflection (in) (mm)	0.003 0.076	0.009 0.229	0.006 0.152	0.007 0.178	0.009 0.229	0.010 0.254	0.011 0.279	0.010 0.254	0.011 0.279	0.009 0.229
Maximum Load (lbf) (N)	260 1157	926 4119	676 3007	810 3603	1120 4982	1122 4991	1217 5413	1189 5289	1217 5413	1162 5169
Ultimate Stress (ksi) (MPa)	46 317	160 1103	118 814	141 972	189 1303	189 1303	202 1393	215 1482	203 1400	205 1413

Table VI. Flexure Test Results for Ultramet-Coated/Ceracon-Consolidated Material

Length (in) **(mm)**	0.5625 14.288	0.5625 14.288	0.5625 14.288	0.5625 14.288	0.5625 14.288	0.5625 14.288	0.5625 14.288
Width (in) **(mm)**	0.1488 3.780	0.1492 3.790	0.1494 3.795	0.1490 3.785	0.1490 3.785	0.1490 3.785	0.1500 3.810
Depth (in) **(mm)**	0.1260 3.200	0.1255 3.188	0.1260 3.200	0.1250 3.175	0.1250 3.175	0.1250 3.175	0.1230 3.124
Composition: %W **%Ni** **%Fe**	94.0 4.3 1.7	94.0 4.3 1.7	94.0 4.3 1.7	94.0 4.3 1.7	94.0 4.3 1.7	94.0 4.3 1.7	94.0 4.3 1.7
Consolidation	Ceracon	Ceracon	Ceracon	Ceracon	Ceracon	Ceracon	Ceracon
Measured Density (g/cm^3)	17.95	17.95	17.95	17.51	17.80	17.95	17.95
Theoretical Density (g/cm^3)	17.95	17.95	17.95	17.95	17.95	17.95	17.95
Percent Dense	100.0	100.0	100.0	97.5	99.2	100.0	100.0
Deflection (in) **(mm)**	0.024 0.610	0.018 0.457	0.020 0.508	0.010 0.254	0.013 0.330	0.016 0.406	0.024 0.610
Maximum Load (lbf) **(N)**	889 3954	801 3563	785 3492	667 2967	810 3603	949 4221	823 3661
Ultimate Stress (ksi) **(MPa)**	318 2193	288 1986	279 1924	242 1669	294 2027	344 2372	306 2110

Table VII. Flexure Test Results for Ultramet/HIP, Ultramet/Ceracon, and Commercial/LPS Material

Length (in) (mm)	0.5625 14.288	0.5625 14.288	0.5625 14.288	0.5625 14.288	0.5625 14.288	0.5625 14.288	0.5625 14.288	0.5625 14.288	0.5625 14.288
Width (in) (mm)	0.1903 4.834	0.1894 4.811	0.1894 4.811	0.1860 4.724	0.1890 4.801	0.1890 4.801	0.1488 3.780	0.1492 3.790	0.1494 3.795
Depth (in) (mm)	0.1630 4.140	0.1590 4.039	0.1590 4.039	0.1490 3.785	0.1500 3.810	0.1500 3.810	0.1260 3.200	0.1255 3.188	0.1260 3.200
Composition: %W **%Ni** **%Fe** **% uncoated 5-μm tungsten powder**	95.3 3.5 1.2 10.0	95.3 3.5 1.2 10.0	95.3 3.5 1.2 10.0	90.0 7.0 3.0 0.0	90.0 7.0 3.0 0.0	90.0 7.0 3.0 0.0	94.0 4.3 1.7 0.0	94.0 4.3 1.7 0.0	94.0 4.3 1.7 0.0
Consolidation	HIP	HIP	HIP	LPS	LPS	LPS	Ceracon	Ceracon	Ceracon
Measured Density (g/cm^3)	18.24	18.24	18.24	17.15	17.15	17.15	17.95	17.95	17.95
Theoretical Density (g/cm^3)	18.24	18.24	18.24	17.15	17.15	17.15	17.95	17.95	17.95
Percent Dense	100	100	100	100	100	100	100	100	100
Deflection (in) (mm)	0.011 0.279	0.009 0.229	0.009 0.229	0.017 0.432	0.015 0.381	0.015 0.381	0.024 0.610	0.018 0.457	0.020 0.508
Maximum Load (lbf) (N)	1217 5413	1162 5169	1169 5200	1000 4448	1111 4942	1059 4711	889 3954	801 3563	785 3492
Ultimate Stress (ksi) (MPa)	203 1400	205 1413	206 1420	204 1407	220 1517	210 1448	318 2193	288 1986	279 1924

Table VIII. Test Data for AMTL Ballistic Testing of Ultramet W_p Composites

Range Test#	Steel	Penetrator	Vs (fps)	Vs (m/s)	Yaw (°)	DOP (in.)	DOP (mm)	CDOP (in)	CDOP (mm)	Comments:
T72-91-1	RHA	Dowding WHA L/D=10; SN 3758-A	4864	1483	2.10	2.756	70.0	2.792	70.9	Str; sym
T72-91-2	RHA	Dowding WHA L/D=10; SN 3760-A	4987	1520	4.22	2.812	71.4	2.725	69.2	Str; sym
T72-91-3	RHA	Dowding WHA L/D=10; SN 3760-B	4963	1513	2.33	2.737	69.5	2.674	67.9	Sl. skew; sym
T72-91-4*	RHA	Dowding WHA L/D=10; SN 3757-A	4930	1503	6.01	2.419	61.4	2.389	60.7	Asym; rough; irreg.; tip pointed
T72-91-5	RHA	Dowding WHA L/D=10; SN 3747-A	4957	1511	2.35	2.854	72.5	2.797	71.0	Sl. skew; sym
T72-91-6	RHA	Dowding WHA L/D=10; SN 3756-A	5156	1572	3.02	3.008	76.4	2.752	69.9	Str; sym
T72-91-7	RHA	Dowding WHA L/D=10; SN 3756-B	4776	1456	1.97	2.559	65.0	2.683	68.1	Str; sym
T72-91-8	RHA	Dowding WHA L/D=10; SN 3757-B	4289	1307	3.18	1.929	49.0	2.540	64.5	Asym; rough; pusher follow
T72-91-9	RHA	Dowding WHA L/D=10; SN 3758-B	4399	1341	1.95	2.263	57.5	2.764	70.2	Str; sym

Distribution List

1 Office of the Secretary of Defense for Research and Engineering, The Pentagon, Washington, D.C. 20301

Commander, U.S. Army Laboratory Command, 2800 Powder Mill Road, Adelphi, MD 20783-1145
1 ATTN: AMSLC-IM-TL
1 ATTN: AMSLC-CT

Commander, Defense Technical Information Center, Cameron Station, Building 5, 5010 Duke Street, Alexandria, VA 22304-6145
2 DTIC-FDAC

1 MIAC/CINDAS, Purdue University, 2595 Yeager Road, West Lafayette, IN 47905

Commander, Army Research Office, P.O. Box 12211, Research Triangle Park, NC
27709-2211
1 ATTN: Information Processing Office
1 Dr. Andrew Crowson
Dr. Edward Chen

Commander U.S. Army Materiel Command (AMC), 5001 Eisenhower Avenue, Alexandria, VA 22333
1 ATTN: AMCSCI

Commander, U.S. Army Materiel Systems Analysis Activity, Aberdeen Proving Ground, MD 21005
1 ATTN: AMXSY-MP, Director

Commander, U.S. Army Missile Command, Redstone Scientific Information Center, Redstone Arsenal, AL 35898-5241
1 ATTN: AMSMI-RD-CS-R/Doc

Commander, U.S. Army Armament Research Development and Engineering Center, Dover, NJ 07801
1 ATTN: Technical Library
1 Mr. D. Kapoor
1 Dr. S. Cytron

Commander, U.S. Army Tank-Automotive Command, Warren, MI 48397-5000
2 ATTN: AMSTA-TSL Technical Library

Commander, U.S. Army Foreign Science and Technology Center, 220 7th Street, N.E., Charlottesville, VA 22901
3 ATTN: AIFRTC, Applied Technologies Branch, Gerald Schlesinger

Naval Research Laboratory, Washington, D.C. 20375
1 ATTN: Code 5830
1 Code 2627

Chief of Naval Research, Arlington, VA 22217
1 ATTN: Code 471

Naval Surface Weapons Center, Dahlgren Laboratory, Dahlgren, VA 22448
1 ATTN: Code G-32, Ammunition Branch, Mr. Brian Sabourin

Commander, Rock Island Arsenal, Rock Island, IL 61299-6000
1 ATTN: SMCRI-SEM-T

Battelle Columbus Laboratories, Battelle Memorial Institute, 505 King Avenue, Columbus, OH 43201
1 ATTN: Mr. Henry Cialone
1 Dr. Alan Clauer

Battelle Pacific Northwest Laboratories, P.O. Box 999, Richland, WA 99352
1 ATTN: Mr. William Gurwell
1 Dr. Gordon Dudder

GTE Sylvania, Inc. Chemical and Metallurgical Division, Hawes Street, Towanda, PA 18848
1 ATTN: Dr. James Mullendore
1 Mr. James Spencer

Director, Ballistic Research Laboratory, Aberdeen Proving Ground, MD 21005
1 ATTN: SLCBR-TSB-S (STINFO)
1 SLCBR-TB-P, Mr. Lee Magness

Teledyne Firth Sterling, 1 Teledyne Place, LaVergne, TN 37086
1 ATTN: Dr. Steven Caldwell
1 Dr. Thomas Penrice

Technology Associates Corp., 17911 Sampson Lane, Huntington Beach, CA
92647
1 ATTN: Dr. Gary Allen

Los Alamos National Laboratory, ATAC, MS F681, P.O. Box 1663, Los Alamos, NM 87545
1 ATTN: Dr. Bill Hogan

Philips Elmet, 1560 Lisbon Road, Lewiston, ME 04240
1 ATTN: Mr. James Anderson

Ultramet, Inc., 12173 Montague Street, Pacoima, CA 91331
1 ATTN: Dr. J.J. Stiglich
1 Mr. Brian Williams
1 Dr. Robert Tuffias

Ceracon, Inc., 1101 N. Market Boulevard, Suite 9, Sacramento, CA 95834
1 ATTN: Dr. Ramas Raman

Southwest Research Institute, 6220 Culebra Road, P.O. Drawer 28510, San Antonio, TX 78228-0510
1 ATTN: Dr. Animesh Bose
1 Dr. James Lankford

Metalworking Technology, Inc., 1450 Scalp Avenue, Johnstown, PA 15904
1 ATTN: Mr. C. Buck Skena
1 Mr. Timothy McCabe

Research Triangle Institute, P.O. Box 12194, Research Triangle Park, NC 27709-2154
1 ATTN: Dr. John B. Posthill

3C Systems, 620 Arglye Road, Wynnewood, PA 19096
1 ATTN: Mr. Murray Kornhauser

Advance Technology Coatings, 300 Blue Smoke Ct. West, Fort Worth, TX 76105
1 ATTN: Mr. Grady Sheek

Alliant Techsystems, 7225 Northland Drive, Brooklyn Park, MN 55428
1 ATTN: Dr. Stan Nelson
1 Mr. MArk Jones
1 Mr. Thomas Steigauf

CAMDEC, 3002 Dow Avenue, Suite 110, Tustin, CA 92680
1 ATTN: Dr. Richard Harlow

Chamberlain Manufacturing Co., 550 Esther St., P.O. Box 2545, Waterloo, IA
50704
1 ATTN: Mr. Tom Lynch

Defense Technology International, Inc., The Stark House, 22 Concord Street,
Nashua, NH
1 ATTN: Mr. Douglas Ayer

Materials and Electrochemical Research Corporation, 7960 S. Kolb Road, Tucson, AZ 85706
1 ATTN: Dr. James Withers
1 Dr. Sumit Guha

Materials Modification, Inc., 2929-P1 Eskridge Center, Fairfax, VA 22031
1 ATTN: Dr. T.S. Sudarshan

Micro Materials Technology, 120-D Research Drive, Milford, CT 06460
1 ATTN: Dr. Richard Cheney

Nuclear Metals, 2229 Main Street, Concord, MA 01742
1 ATTN: Dr. Willian Nachtrab

Olin Ordnance, 10101 9th Street N., St. Petersburg, FL
1 ATTN: Hugh McElroy

The Pennsylvania State University, Department of Engineering Science and Mechanics, 227 Hammond Building, University Park, PA 16802-1401
1 ATTN: Dr. Randall M. German, Professor, Brush Chair in Materials

Director, U.S. Army Materials Technology Laboratory, Watertown, MA 02172-0001
2 ATTN: SLCMT-TML
1 SLCMT-IMA-V
1 SLCMT-PRC
20 SLCMT-MEM, Mr. Robert Dowding

U.S. Army Materials Technology Laboratory, Watertown, Massachusetts 02172-0001
COATED TUNGSTEN POWDERS FOR ADVANCED ORDNANCE APPLICATIONS, PHASE II, SBIR - Brian E. Williams, Jacob J. Stiglich, Jr., and Richard B. Kaplan
Ultramet, Pacoima, CA 91331

Technical Report MTL TR 92-35, May 1992, 67 pp - illus-tables, Contract DAAL04-88-C-0030
Final Report, Sep 88 to Jul 91

AD ____________

UNCLASSIFIED
UNLIMITED DISTRIBUTION

Key Words

Tungsten powder
Composites
Chemical vapor deposition (CVD)

In this program, Ultramet optimized and characterized a fluidized-bed chemical vapor deposition (CVD) process for depositing nickel and iron onto tungsten particles for potential use as kinetic energy penetrator materials. The process yields a composite powder having the nominal composition W-6%Ni/Fe, in which the Ni:Fe ratio is 7:3. Two relatively narrow tungsten particle size distributions were used: one with a mean size of 12-15 μm, the other with a mean size of 5 μm. These particle sizes facilitated fluidized-bed CVD processing, but limited the ability to consolidate the materials by liquid phase sintering (LPS). Consequently, solid-state consolidation (Ceracon® process) was used to fabricate billets from which flexure, tensile, impact, and quarter-scale ballistic specimens could be machined. Initial three-point flexure measurements were very encouraging, with modulus-of-rupture values 30-50% higher than those of commercial (90:10, LPS) material cut into similar bars and tested concurrently, and midspan deflections equal to those of the (usually) more ductile 90:10 material. The tensile, impact, and ballistic properties of specimens fabricated from larger billets, however, did not reproduce the earlier flexure results. Tensile strengths were respectable, but ductility was limited to ≤1% elongation. This brittleness was borne out in impact testing and in ballistic testing against spaced plate targets, although ballistic testing against semi-infinite rolled homogeneous armor at 0° obliquity yielded results identical to those for commercial and experimental tungsten composites of comparable density (tungsten content).

U.S. Army Materials Technology Laboratory, Watertown, Massachusetts 02172-0001
COATED TUNGSTEN POWDERS FOR ADVANCED ORDNANCE APPLICATIONS, PHASE II, SBIR - Brian E. Williams, Jacob J. Stiglich, Jr., and Richard B. Kaplan
Ultramet, Pacoima, CA 91331

Technical Report MTL TR 92-35, May 1992, 67 pp - illus-tables, Contract DAAL04-88-C-0030
Final Report, Sep 88 to Jul 91

AD ____________

UNCLASSIFIED
UNLIMITED DISTRIBUTION

Key Words

Tungsten powder
Composites
Chemical vapor deposition (CVD)

In this program, Ultramet optimized and characterized a fluidized-bed chemical vapor deposition (CVD) process for depositing nickel and iron onto tungsten particles for potential use as kinetic energy penetrator materials. The process yields a composite powder having the nominal composition W-6%Ni/Fe, in which the Ni:Fe ratio is 7:3. Two relatively narrow tungsten particle size distributions were used: one with a mean size of 12-15 μm, the other with a mean size of 5 μm. These particle sizes facilitated fluidized-bed CVD processing, but limited the ability to consolidate the materials by liquid phase sintering (LPS). Consequently, solid-state consolidation (Ceracon® process) was used to fabricate billets from which flexure, tensile, impact, and quarter-scale ballistic specimens could be machined. Initial three-point flexure measurements were very encouraging, with modulus-of-rupture values 30-50% higher than those of commercial (90:10, LPS) material cut into similar bars and tested concurrently, and midspan deflections equal to those of the (usually) more ductile 90:10 material. The tensile, impact, and ballistic properties of specimens fabricated from larger billets, however, did not reproduce the earlier flexure results. Tensile strengths were respectable, but ductility was limited to ≤1% elongation. This brittleness was borne out in impact testing and in ballistic testing against spaced plate targets, although ballistic testing against semi-infinite rolled homogeneous armor at 0° obliquity yielded results identical to those for commercial and experimental tungsten composites of comparable density (tungsten content).

U.S. Army Materials Technology Laboratory, Watertown, Massachusetts 02172-0001
COATED TUNGSTEN POWDERS FOR ADVANCED ORDNANCE APPLICATIONS, PHASE II, SBIR - Brian E. Williams, Jacob J. Stiglich, Jr., and Richard B. Kaplan
Ultramet, Pacoima, CA 91331

Technical Report MTL TR 92-35, May 1992, 67 pp - illus-tables, Contract DAAL04-88-C-0030
Final Report, Sep 88 to Jul 91

AD ____________

UNCLASSIFIED
UNLIMITED DISTRIBUTION

Key Words

Tungsten powder
Composites
Chemical vapor deposition (CVD)

In this program, Ultramet optimized and characterized a fluidized-bed chemical vapor deposition (CVD) process for depositing nickel and iron onto tungsten particles for potential use as kinetic energy penetrator materials. The process yields a composite powder having the nominal composition W-6%Ni/Fe, in which the Ni:Fe ratio is 7:3. Two relatively narrow tungsten particle size distributions were used: one with a mean size of 12-15 μm, the other with a mean size of 5 μm. These particle sizes facilitated fluidized-bed CVD processing, but limited the ability to consolidate the materials by liquid phase sintering (LPS). Consequently, solid-state consolidation (Ceracon® process) was used to fabricate billets from which flexure, tensile, impact, and quarter-scale ballistic specimens could be machined. Initial three-point flexure measurements were very encouraging, with modulus-of-rupture values 30-50% higher than those of commercial (90:10, LPS) material cut into similar bars and tested concurrently, and midspan deflections equal to those of the (usually) more ductile 90:10 material. The tensile, impact, and ballistic properties of specimens fabricated from larger billets, however, did not reproduce the earlier flexure results. Tensile strengths were respectable, but ductility was limited to ≤1% elongation. This brittleness was borne out in impact testing and in ballistic testing against spaced plate targets, although ballistic testing against semi-infinite rolled homogeneous armor at 0° obliquity yielded results identical to those for commercial and experimental tungsten composites of comparable density (tungsten content).

U.S. Army Materials Technology Laboratory, Watertown, Massachusetts 02172-0001
COATED TUNGSTEN POWDERS FOR ADVANCED ORDNANCE APPLICATIONS, PHASE II, SBIR - Brian E. Williams, Jacob J. Stiglich, Jr., and Richard B. Kaplan
Ultramet, Pacoima, CA 91331

Technical Report MTL TR 92-35, May 1992, 67 pp - illus-tables, Contract DAAL04-88-C-0030
Final Report, Sep 88 to Jul 91

AD ____________

UNCLASSIFIED
UNLIMITED DISTRIBUTION

Key Words

Tungsten powder
Composites
Chemical vapor deposition (CVD)

In this program, Ultramet optimized and characterized a fluidized-bed chemical vapor deposition (CVD) process for depositing nickel and iron onto tungsten particles for potential use as kinetic energy penetrator materials. The process yields a composite powder having the nominal composition W-6%Ni/Fe, in which the Ni:Fe ratio is 7:3. Two relatively narrow tungsten particle size distributions were used: one with a mean size of 12-15 μm, the other with a mean size of 5 μm. These particle sizes facilitated fluidized-bed CVD processing, but limited the ability to consolidate the materials by liquid phase sintering (LPS). Consequently, solid-state consolidation (Ceracon® process) was used to fabricate billets from which flexure, tensile, impact, and quarter-scale ballistic specimens could be machined. Initial three-point flexure measurements were very encouraging, with modulus-of-rupture values 30-50% higher than those of commercial (90:10, LPS) material cut into similar bars and tested concurrently, and midspan deflections equal to those of the (usually) more ductile 90:10 material. The tensile, impact, and ballistic properties of specimens fabricated from larger billets, however, did not reproduce the earlier flexure results. Tensile strengths were respectable, but ductility was limited to ≤1% elongation. This brittleness was borne out in impact testing and in ballistic testing against spaced plate targets, although ballistic testing against semi-infinite rolled homogeneous armor at 0° obliquity yielded results identical to those for commercial and experimental tungsten composites of comparable density (tungsten content).